JPn Neuroscience

The Journal of Physiology

J Physiol 591.22 (2013) pp 5555–5574

Stomatin-domain protein interactions with acid-sensing ion channels modulate nociceptor mechanosensitivity

Rabih A. Moshourab, Christiane Wetzel, Carlos Martinez-Salgado and Gary R. Lewin

Department of Neuroscience, Max-Delbrück Center for Molecular Medicine and Charité Universitätsmedizin Berlin, Robert-Rössle-Straße 10, Berlin-Buch D-13125, Germany

Key points

- Gene deletion studies revealed that membrane proteins stomatin and STOML3, as well as the acid-sensing ion channels ASIC2 and ASIC3, regulate mechanosensory transduction.
- Both stomatin and STOML3 interact with ASIC proteins and we asked if deletion of two interacting proteins has a more than additive effect on the mechanosensitivity of cutaneous sensory afferents.
- A detailed electrophysiological comparison of sensory afferent phenotypes observed in *asic3*$^{-/-}$:*stomatin*$^{-/-}$, *asic3*$^{-/-}$:*stoml3*$^{-/-}$ and *asic2*$^{-/-}$:*stomatin*$^{-/-}$ mutant mice compared to their respective single gene mutants revealed especially strong effects on the mechanosensitivity of thinly myelinated mechanonociceptors in double mutants.
- Deletion of the *asic3* gene or pharmacological blockade of this channel decreased adaptation rates specifically in rapidly adapting mechanoreceptors, an effect not exacerbated by deletion of stomatin-domain genes.
- This study reveals that loss of stomatin–ASIC interactions can have profound effects on mechanosensitivity in specific subsets of skin afferents; interfering with such interactions could have potential for treating mechanical pain.

Abstract Acid-sensing ion channels (ASICs) and their interaction partners of the stomatin family have all been implicated in sensory transduction. Single gene deletion of *asic3*, *asic2*, *stomatin*, *or stoml3* all result in deficits in the mechanosensitivity of distinct cutaneous afferents in the mouse. Here, we generated *asic3*$^{-/-}$:*stomatin*$^{-/-}$, *asic3*$^{-/-}$:*stoml3*$^{-/-}$ and *asic2*$^{-/-}$:*stomatin*$^{-/-}$ double mutant mice to characterize the functional consequences of stomatin–ASIC protein interactions on sensory afferent mechanosensitivity. The absence of ASIC3 led to a clear increase in mechanosensitivity in rapidly adapting mechanoreceptors (RAMs) and a decrease in the mechanosensitivity in both Aδ- and C-fibre nociceptors. The increased mechanosensitivity of RAMs could be accounted for by a loss of adaptation which could be mimicked by local application of APETx2 a toxin that specifically blocks ASIC3. There is a substantial loss of mechanosensitivity in *stoml3*$^{-/-}$ mice in which ∼35% of the myelinated fibres lack a mechanosensitive receptive field and this phenotype was found to be identical in *asic3*$^{-/-}$:*stoml3*$^{-/-}$ mutant mice. However, Aδ-nociceptors showed much reduced mechanosensitivity in *asic3*$^{-/-}$:*stoml3*$^{-/-}$ mutant mice compared to *asic3*$^{-/-}$ controls. Interestingly, in *asic2*$^{-/-}$:*stomatin*$^{-/-}$ mutant mice many Aδ-nociceptors completely lost their mechanosensitivity which was not observed in *asic2*$^{-/-}$ or *stomatin*$^{-/-}$ mice. Examination of *stomatin*$^{-/-}$:*stoml3*$^{-/-}$ mutant mice indicated that a stomatin/STOML3 interaction is unlikely to account for the greater Aδ-nociceptor deficits in double mutant mice. A key finding from these studies is that the loss of stomatin or STOML3

R. A. Moshourab and C. Wetzel contributed equally to this work.

DOI: 10.1113/jphysiol.2013.261180

in *asic3*$^{-/-}$ or *asic2*$^{-/-}$ mutant mice markedly exacerbates deficits in the mechanosensitivity of nociceptors without affecting mechanoreceptor function.

(Received 26 June 2013; accepted after revision 18 August 2013; first published online 19 August 2013)
Corresponding author G. R. Lewin: Department of Neuroscience, Max-Delbrück Center for Molecular Medicine, Robert-Rössle Str. 10, D-13125, Berlin, Germany. Email: glewin@mdc-berlin.de

Abbreviations AM, Aδ-fibre mechanonociceptor; APETx2, *Anthopleura elegantissima* toxin; ASIC, acid-sensing ion channel; C-M, C-mechanonociceptor; C-MH, C-mechanoheat unit; CV, conduction velocity; Deg/ENaC, degenerin/epithelial sodium channel superfamily; D-hair, down hair; RAM, rapidly adapting mechanoreceptor; SAM, slowly adapting mechanoreceptor; SIF, synthetic interstitial fluid; STOML3, stomatin-domain protein 3; vFT, von Frey threshold.

Introduction

Stomatin and STOML3 are closely related integral membrane proteins that play important roles in the sensory mechanotransduction (Wetzel *et al.* 2007; Martinez-Salgado *et al.* 2007). Deletion of the STOML3 gene in mice leads to a complete loss of mechanosensitivity in many cutaneous afferents, and a concomitant loss of mechanosensitive currents (Wetzel *et al.* 2007). Deletion of the stomatin gene has mild effects on the sensitivity of mechanoreceptors called down hair (D-hair) receptors (Lewin & Moshourab, 2004; Martinez-Salgado *et al.* 2007; Wang & Lewin, 2011; Lechner & Lewin, 2013). Both STOML3 and stomatin can interact with acid-sensing ion channels (ASICs) and function to suppress the magnitude and modulate the inactivation kinetics of proton-gated currents carried by recombinant ASICs (Price *et al.* 2004; Wetzel *et al.* 2007; Lapatsina *et al.* 2012*b*; Brand *et al.* 2012). ASIC3 in particular is an important proton sensor in sensory neurons but can also regulate the mechanosensitivity of sensory afferents (Price *et al.* 2001; Benson *et al.* 2002; Chen *et al.* 2002; Page *et al.* 2004; Yagi *et al.* 2006; Sluka *et al.* 2007). All five mammalian ASIC isoforms (ASIC1a, ASIC1b, ASIC2a, ASIC2b and ASIC3) are found in dorsal root ganglion (DRG) neurons and these ion channels belong to the degenerin/epithelial sodium channel (Deg/ENaC) superfamily (Arnadóttir & Chalfie, 2010; Smith *et al.* 2011). Three members of the Deg/ENaC family, MEC-4, MEC-10 and DEG-1, have been shown to form a mechanosensitive channel in body and nose touch neurons in the nematode *C. elegans* (Driscoll & Chalfie, 1991; Suzuki *et al.* 2003; O'Hagan *et al.* 2005; Geffeney *et al.* 2011; Geffeney & Goodman, 2012). Interestingly, the activity of MEC-4-containing ion channels is critically dependent on the nematode stomatin-domain protein MEC-2 (Huang *et al.* 1995; Goodman *et al.* 2002; Zhang *et al.* 2004; O'Hagan *et al.* 2005). It is clear that genetic disruption of the *asic1*, *asic2 and asic3* genes leads to alterations in the mechanosensitive properties of a variety of both somatic and visceral sensory neurons (Price *et al.* 2000, 2001; Page *et al.* 2005, 2007; Kang *et al.* 2012). However, the ablation of *asic* channel genes does not appear to impact on mechanosensitive currents in DRG neurons of mice (Drew *et al.* 2004; Lechner *et al.* 2009). The mechanisms that underlie alterations in the stimulus–response properties of sensory neurons in *asic* mutant mice thus remain unknown.

ASIC3- and ASIC2-containing channels can be modulated by both STOML3 and stomatin and physical interactions are observed between all three of these proteins (Price *et al.* 2004; Wetzel *et al.* 2007; Lapatsina *et al.* 2012*b*; Brand *et al.* 2012). We thus reasoned that important functional interactions may be revealed by comparing the mechanosensitivity of cutaneous afferents in a series of double mutant mice, namely *asic3*$^{-/-}$:*stomatin*$^{-/-}$, *asic3*$^{-/-}$:*stoml3*$^{-/-}$, *asic2*$^{-/-}$:*stomatin*$^{-/-}$ and *stomatin*$^{-/-}$:*stoml3*$^{-/-}$ mutant mice. A key finding from these studies is that the loss of stomatin or STOML3 in *asic3*$^{-/-}$ or *asic2*$^{-/-}$ mutant mice markedly exacerbates deficits in the mechanosensitivity of nociceptors in the absence of changes in mechanoreceptor function.

Methods

Generation of mutant mice

The experiments in this study were carried out either on inbred C57BL/6N mice (obtained from Charles River, Sulzfeld, Germany) or on a laboratory-bred hybrid mouse strain. The *asic3*$^{-/-}$ mutant mice were originally a gift from Michael Welsh, Howard Hughes Medical Institute, Iowa, USA, and *stomatin*$^{-/-}$ mutant mice were a gift from Narla Mohandas, Lawrence Berkeley Laboratory, San Francisco, USA. *Stoml3*$^{-/-}$ mice were generated as previously described (Wetzel *et al.* 2007). Crossing *asic3*$^{+/-}$ with *stomatin*$^{+/-}$ or *stoml3*$^{+/-}$ mice generated *asic3*$^{-/-}$:*stomatin*$^{-/-}$ and *asic3*$^{-/-}$:*stoml3*$^{-/-}$ double mutant mice, respectively. Similarly, crossing *stomatin*$^{+/-}$ with *stoml3*$^{+/-}$ mice generated *stoml3*$^{-/-}$:*stomatin*$^{-/-}$ mice. At the time of their analysis, the mutant mice described above were on a C57BL/6N background after back-crossing for at least eight generations. In the case of mice with an *asic2*$^{-/-}$:*stomatin*$^{-/-}$ genotype the strain was only back-crossed onto a pure C57BL/6N background for three generations. Thus, for this double mutant mouse, comparisons were made with the control *asic2*$^{+/+}$:*stomatin*$^{+/+}$ strain obtained from the same breeding programme. There was no indication from our studies here or elsewhere that the phenotypes of sensory

afferents in this control strain differed from that of C57BL/6N mice (Milenkovic *et al.* 2008). All genotyping was carried out with allele-specific genomic PCR. Hybrid wild-type mice were derived from the progeny of multiple intercrosses of mice derived from C57BL/6N–129/Sv chimeric mice as was the *asic2*$^{-/-}$:*stomatin*$^{+/+}$ mice to which they were also compared. Animal housing and care, as well as protocols for humane killing, were registered with and approved by the appropriate German federal authorities (State of Berlin).

In vitro skin–nerve preparation

The skin–nerve preparation was used essentially as previously described to record from single primary afferents (Milenkovic *et al.* 2007, 2008). Mice were killed by CO_2 inhalation for 2–4 min followed by cervical dislocation. The method of killing was approved by the Berlin state authorities responsible for animal welfare. The saphenous nerve and the shaved skin of the hind limb were dissected free and placed in an organ bath. The chamber was perfused with a synthetic interstitial fluid (SIF buffer), the composition of which was (in mM): NaCl, 123; KCl, 3.5; $MgSO_4$, 0.7; NaH_2PO_4, 1.7; $CaCl_2$, 2.0; sodium gluconate, 9.5; glucose, 5.5; sucrose, 7.5; and Hepes, 10 at a pH of 7.4. The skin was placed with the dermis side up in the organ bath. The nerve was placed in an adjacent chamber on a mirror to aid fibre teasing under microscopy. All experiments were carried out with an organ bath temperature of 32°C.

Characterization of single units

Fine filaments were teased from the saphenous nerve and placed on the recording electrode. Electrical isolation was achieved with mineral oil. Single units were identified by gentle mechanical stimulation of their receptive field with a glass rod. Mechanically evoked spikes were visualized and the template saved in an oscilloscope. Then, a sharp tungsten metal electrode was placed in the receptive field and an electrically evoked spike was elicited with suprathreshold current pulses and the electrical latency, the time from the stimulation artifact to spike, was recorded. The distance between the stimulating and recording electrode was designated as the conduction distance. For each isolated fibre the conduction velocity was calculated by dividing conduction distance by electrical latency for the spike. Next the mechanical threshold was estimated by evoking spikes with a series of calibrated von Frey filaments produced bending forces from 0.4 mN to 32 mN. The calibrated von Frey filaments used had the following forces (in mN): 0.4, 1.0, 1.4, 2.0, 3.3, 6.3, 10, 13, 22, 28, 32.

Mechanical stimulation

A computer-controlled nanomotor (Kleindiek, Reutlingen, Germany) was used to apply controlled displacement stimuli of known amplitude and velocity. Standardized displacement stimuli of 10 s duration were applied to the receptive field at regular intervals (interstimulus period, 30 s). The probe was a stainless steel metal rod and the diameter of the flat circular contact area was 0.8 mm as in previous studies (Wetzel *et al.* 2007; Martinez-Salgado *et al.* 2007; Milenkovic *et al.* 2007, 2008). The signal driving the movement of the linear motor and raw electrophysiological data were collected with a Powerlab 4.0 system (ADInstruments) and spikes were discriminated off-line with the spike histogram extension of the software.

The computer-controlled nanomotor was placed onto a spot within the receptive field where the most reliable responses could be obtained with a von Frey filament. Using small movements (48 μm) of the nanomotor the mechanical stimulus was advanced onto the receptive field until one spike was evoked. The amplitude of the stimulus was then systematically reduced and the probe moved into a *z*-axis position, so that the smallest stimulus possible (usually 10 μm) reliably evoked at least one spike when the probe was advanced. The starting position of the mechanical stimulator was therefore just below threshold for each recorded unit.

Two mechanical stimulation protocols were employed. The first protocol consisted of an ascending series of displacement stimuli, sent as a pre-programmed series of commands to the nanomotor. The magnitude of the displacements was between 10 and 800 μm. The standard ramp speed used in the ascending series had a constant velocity of 1435 μm s^{-1}. This protocol was mainly employed on slowly adapting mechanoreceptors (SAMs), Aδ-mechanonociceptors (AMs) and C-fibres, all fibres with predominantly static responses. The second protocol consisted of displacements of 48, 96 or 144 μm with increasing velocities from 1.5 μm s^{-1} up to a maximum of 2945 μm s^{-1}. This protocol was mainly applied on RAM and D-hairs, i.e. rapidly adapting receptors with sensitivity to changes in velocity (Milenkovic *et al.* 2008; Heidenreich *et al.* 2012; Lechner & Lewin, 2013). Mechanical latency was measured for each individual recorded afferent by measuring the delay between the onset of each ramp stimulus and the first spike minus the conduction delay measured.

To test the heat responsiveness of the mechanosensitive C-fibres, preheated SIF buffer was applied on the receptive field isolated with a small metal ring and the actual temperature of the surface of the skin was measured with a thermocouple. All experiments were carried out blind to the animal's genotype.

It is conceivable that changes in mechanoreceptor or nociceptor responses might result from changes in the mechanical properties of the skin, e.g. elasticity or compliance. In most experiments we did not measure the force but used calibrated displacement stimuli. However, we did measure the rate of rise of force using a force measurement device attached to the nanomotor in the skin nerve preparation from C57BL/6N control mice and skin from *asic3*$^{-/-}$:*stoml3*$^{-/-}$ mice and found no differences (data not shown).

Pharmacology

We tested the effects of *Anthopleura elegantissima* toxin (APETx2; Alomone Labs P.O. Box 4287 Jerusalem, Israel) on the response properties of rapidly and slowly adapting mechanoreceptors. Single units were mechanically stimulated with the same probe (0.8 mm diameter) mounted on a piezo device (Physik Instrumente Auf der Römerst, 1 Karlsruhe, Germany (PI)) and controlled by the built-in stimulator function of LabChart 7.1 (ADInstruments). Displacements of 100 μm were delivered with velocities of 450 μm s^{-1} and 1500 μm s^{-1} with 200 and 70 ms ramp-phase durations, respectively. The baseline stimulation consisted of the two 450 and 1500 μm s^{-1} stimuli delivered every 30 s and this was repeated a total of 3 times to rule out response variability. One hundred microlitres of 5 μM APETx2 in oxygenated SIF buffer solution was applied for at least 10 min to the isolated receptive field within a stainless steel ring and the unit was mechanically stimulated at regular intervals during this period. After 10 min exposure to APETx2 drug washout commenced and the receptive field mechanically stimulated at 15, 30 and 60 min. Drug application sites on the skin were marked to avoid exposing the same area of skin to the drug more than once.

Analysis of RAM adaptation

The spike sequences were aligned with the onset of the first spike to normalize for mechanical latency. The movement phase of the 122 μm s^{-1}, 530 μm s^{-1} and 1020 μm s^{-1} stimulus was divided into bins of 100 ms, 50 ms and 20 ms, respectively (Fig. 1*C*–*E*). The number of spikes falling in these bins was counted for the whole population of RAMs and a spike histogram was generated for each mutant mouse genotype. The cumulative distribution of spikes was then fitted with an exponential decay function ($y = Ae^{-bx}$). Thus, we could calculate the time constant τ as a measure of adaptation during the ramp.

Immunostaining of tissue sections

Mice were anaesthetized with 0.1 mg ml^{-1} sodium urethane (0.1–0.5 ml or more injected intra-perotoneal route) and perfused intracardially with 4% paraformaldehyde in 0.1 M PBS, pH 7.4 and 4°C. Immediately after perfusion the skin was dissected and post-fixed in the perfusion fixative at 4°C for 4 h.

Tissue was immersed in 25% sucrose in PBS for 1–3 days until the skin sank to the bottom of the sucrose solution. Fresh sucrose solution was replaced daily.

Skin sections were cut on a freezing microtome into 40 μm sections perpendicular to the skin surface. Skin sections were pre-incubated in 1% bovine serum albumin and 0.3% Triton X-100 in Tris-buffered saline (TBS) for 1 h and incubated overnight at room temperature with a protein gene product 9.5 (PGP9.5) PGP 9.5 antibody (RA15101; Ultra Clone Ltd, Isle of Wight, UK), diluted 1:2000 in TBS with 0.3% Triton X-100 and 5% normal goat serum. Skin sections were washed by rinsing slides in excess TBS for 30 min and incubated for 1 h at room temperature with Cy-3-conjugated secondary antibodies diluted 1:800 in TBS containing 0.3% Triton X-100 and 5% normal goat serum. Skin sections were washed twice in excess TBS for 30 min and then once with water before mounting them in Aqua-Polymount (polysciences Inc. Eppenheim, Germany. Cy3 light emission was captured with the XF22 filter (excitation 535 nm, emission 605DF50, Omega Optical).

Electron microscopy

After induction of deep anesthesia with an intra-perotoneal dose of sodium urethane 0.1 mg ml^{-1} mice were perfused with freshly prepared 4% formaldehyde in 0.1 M phosphate buffer. Saphenous nerves were dissected and post-fixed in 4% formaldehyde–2.5% glutaraldehyde in 0.1 M phosphate buffer for 3 days. Following treatment with 1% OsO_4 for 2 h, they were dehydrated in a graded ethanol series and propylene oxide and embedded in Poly/Bed 812 (Polysciences, Inc., Eppelheim, Germany). Semi-thin sections were stained with toluidine blue. Ultrathin sections (70 nm) were contrasted with uranyl acetate and lead citrate and examined with a Zeiss 910 electron microscope (St John Smith *et al.* 2012).

Digital images were taken with a 1k × 1k pixel high-speed slow scan CCD camera (Proscan) at an original magnification of ×1600. Two ultrathin sections per nerve and genotype were analysed. On each ultrathin section, four images were taken representing an area of 18.25 μm × 18.27 μm. Myelinated and non-myelinated axons were counted on these areas using the analySIS 3.2 software (Soft Imaging System, Münster, Germany), and normalized to the whole nerve. Imaging and analysis was done with the help of Bettina Purfürst at the MDC electron microscopy core facility as previously documented (St John Smith *et al.* 2012).

Statistical analysis

The recording and analysis for each mechanosensitive afferent unit included the four parameters: (1) conduction velocity (CV); (2) mechanical activation threshold (von Frey threshold, vFT); (3) stimulus–response function; and (4) mechanical latency. For construction of the stimulus–response functions spikes discharged during the 10 s stimulus were counted using LabChart with

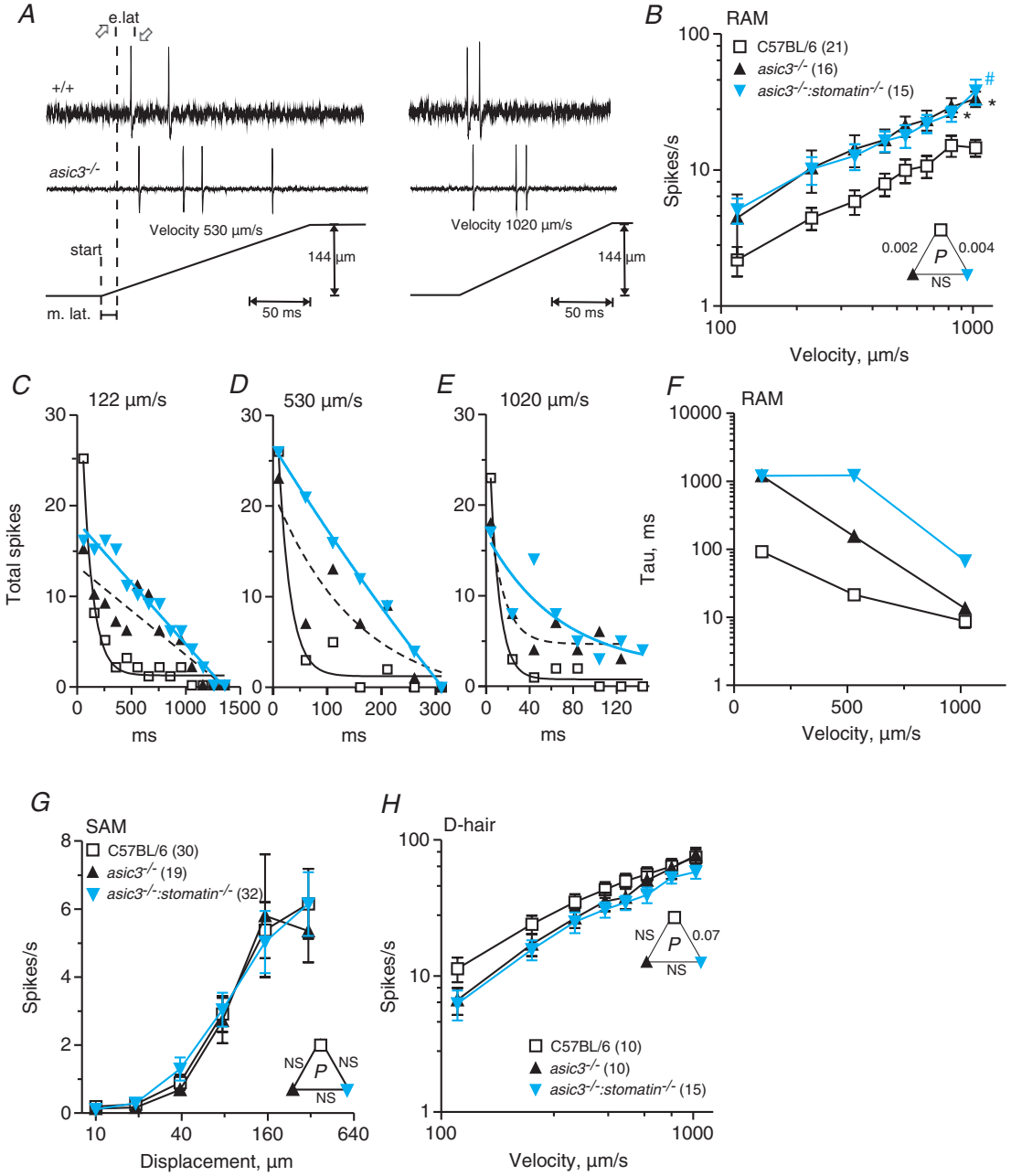

Figure 1. Low threshold mechanoreceptors in control, *asic3*$^{-/-}$ and *asic3*$^{-/-}$:*stomatin*$^{-/-}$ mice
A, illustration of a typical response of a RAM to stimuli of increasing velocity. Spikes occur exclusively during the ramp phase after a short latency, e.lat and m.lat are abbreviations for electrical and mechanical latency, respectively. *B*, responses of RAMs from *asic3*$^{-/-}$ and *asic3*$^{-/-}$:*stomatin*$^{-/-}$ are increased compared to control ($P < 0.05$, repeated measures ANOVA). *C*, *D* and *E* show cumulative response of all RAM units during ramp phase of stimulus. These were fitted to a one-phase decay exponential function to derive the time constants 'τ'. *F*, the derived 'τ' for each mutant mouse plotted against stimulus velocity show slower adaptation in mutant mice. *G* and *H*, stimulus–response plots of SAM and D-hairs were unaltered compared to controls. Error bars indicate SEM. **P* < 0.05, Bonferroni *post hoc* test *asic3*$^{-/-}$ *vs.* control. #*P* < 0.05, Bonferroni *post hoc* test *asic3*$^{-/-}$:*stomatin*$^{-/-}$ *vs.* control.

spike histogram extension software. Stimulus–response functions for each receptor type were compared between mouse strains using repeated measures ANOVA. A Bonferroni *post hoc* test was used if ANOVA revealed a significant effect. To calculate the rate of adaptation during the ramp phase of the mechanical stimulus the spikes were binned with the first histogram normalized to the first spike after stimulus onset for each unit. Spike discrimination was done with the spike discriminator module of the Chart program version 4 provided by ADInstruments. Statistical analysis and exponential fits were made using the Graphpad Prism software.

Results

Sample and mouse strains

A total of 2090 single afferent units studied from the saphenous nerve of wild-type mice ($n = 44$) and *asic3*$^{-/-}$ ($n = 9$), *asic3*$^{-/-}$:*stomatin*$^{-/-}$ ($n = 21$), *asic3*$^{-/-}$:*stoml3*$^{-/-}$ ($n = 15$), *stomatin*$^{-/-}$:*stoml3*$^{-/-}$ ($n = 13$); *asic2*$^{-/-}$:*stomatin*$^{-/-}$ ($n = 17$) and *asic2*$^{-/-}$ ($n = 9$) mice. *Stomatin*$^{-/-}$ and *stoml3*$^{-/-}$ mice were previously studied in detail using the same methodology (Wetzel *et al.* 2007; Martinez-Salgado *et al.* 2007). The wild-type mice used were either pure C57BL/6N or a hybrid mouse strain which is a mixture of 129/Sv and C57BL/6N and data from these mice referred to here as *asic2*$^{+/+}$:*stomatin*$^{+/+}$ were only compared to those from *asic2*$^{-/-}$:*stomatin*$^{-/-}$ mice which had an identical genetic background. A summary of the sensory receptor subtypes, including mean conduction velocity and mechanical thresholds of the mutant mice types, is shown in Tables 1 and 2.

Proportion of mechanically insensitive units in *asic3*$^{-/-}$:*stomatin*$^{-/-}$, *asic3*$^{-/-}$:*stoml3*$^{-/-}$ and *stomatin*$^{-/-}$:*stoml3*$^{-/-}$ double mutant mice

We asked if the absence of any two of the three proteins ASIC3, stomatin and STOML3 would render sensory afferents insensitive to mechanical stimuli. Using an electrical search strategy, the incidence of mechanically insensitive units was determined in double mutant mice (Table 1). For just 11 of 159 electrically identified units in controls we could find no mechanosensitive receptive field, so-called mechanoinsensitive fibres. Similarly, the proportions of mechanically insensitive units in *asic3*$^{-/-}$ (2/38) and *asic3*$^{-/-}$:*stomatin*$^{-/-}$ (7/74) mice did not significantly differ for all receptor types and subtypes when compared to wild-type controls (Table 1, $P > 0.05$, Fisher's exact test). In contrast, a significantly higher proportion (19/77) of units had no mechanosensitive receptive fields in *asic3*$^{-/-}$:*stoml3*$^{-/-}$ mice compared to control ($P < 0.005$, Fisher's exact test). The same trend was observed for *stomatin*$^{-/-}$:*stoml3*$^{-/-}$ mutants (Table 1). A significant proportion of Aβ and Aδ-fibres were mechanoinsensitive in both *asic3*$^{-/-}$:*stoml3*$^{-/-}$ and *stomatin*$^{-/-}$:*stoml3*$^{-/-}$ mutants compared to controls ($P < 0.05$, Fisher's exact test). Since the proportion of mechanically insensitive afferents found in both *asic3*$^{-/-}$:*stoml3*$^{-/-}$ and *stomatin*$^{-/-}$:*stoml3*$^{-/-}$ mutants was very similar to that already found for *stoml3*$^{-/-}$ mutants alone (Wetzel *et al.* 2007), we thus conclude that the loss of mechanosensitivity probably results from the absence of STOML3 alone and is not due to a loss of interaction between STOML3 and ASIC3 or stomatin and ASIC3.

Properties of mechanoreceptors in *asic3*$^{-/-}$:*stomatin*$^{-/-}$ double mutant mice

We confirmed that the vast majority of Aβ-fibres had a mechanosensitive receptive field in the skin of control wild-type (95% 69/73 fibres), *asic3*$^{-/-}$ (100% 11/11 fibres) and *asic3*$^{-/-}$:*stomatin*$^{-/-}$ (93% 25/27 fibres) mice. In the original description of mechanoreceptors in *asic3*$^{-/-}$ mice we described an apparent hypersensitivity of rapidly adapting mechanoreceptors (RAMs), but not of slowly adapting mechanoreceptors (SAMs) (Price *et al.* 2001). However, in earlier studies the mechanosensitivity was not tested with a computer-controlled stimulus and the exact velocity sensitivity of the mechanoreceptors could not be determined. Here we used a series of constant amplitude ramp-and-hold stimuli in which the speed of the ramp was systematically varied from 100 μm s^{-1} to 1000 μm s^{-1}. In controls the spike rate increased with velocity and this was also true of RAMs in *asic3*$^{-/-}$ mice. However, the absolute firing rate of RAMs in *asic3*$^{-/-}$ mice was more than twice as large as control RAMs at all velocities tested ($P < 0.005$, repeated measures ANOVA with Bonferroni *post hoc* tests; Fig. 1*B*). We repeated the same analysis of RAMs in *asic3*$^{-/-}$:*stomatin*$^{-/-}$ mutants and found that this hypersensitivity effect was identical to that of RAMs in *asic3*$^{-/-}$ single mutant mice ($P > 0.05$, repeated measures ANOVA; Fig. 1*B*). We determined the characteristics of the increased responses by examining the discharge pattern of RAMs to increasing velocity stimulation. RAMs discharge at a high frequency at the beginning of the ramp but show adaptation during the ramp so that spike frequency is lower toward the end of the ramp. As can be seen in the example records the increased firing rates of RAMs in *asic3*$^{-/-}$ single and *asic3*$^{-/-}$:*stomatin*$^{-/-}$ double mutant mice were associated with a much slower rate of adaptation, τ, calculated as described in the Methods (Fig. 1*A*). We found a substantial increase of over 100-fold in τ in *asic3*$^{-/-}$ as well as *asic3*$^{-/-}$:*stomatin*$^{-/-}$ mutants compared to controls (Fig. 1*F*). The changes in RAM

Table 1. Properties of sensory receptor subtypes in controls, *asic3*$^{-/-}$, *asic3*$^{-/-}$:*stomatin*$^{-/-}$, *stomatin*$^{-/-}$:*stoml3*$^{-/-}$ and *asic3*$^{-/-}$:*stoml3*$^{-/-}$ mutant mice

Mechanical search			Controls	*asic3*$^{-/-}$	*stomatin*$^{-/-}$:*stoml3*$^{-/-}$	*asic3*$^{-/-}$:*stomatin*$^{-/-}$	*asic3*$^{-/-}$:*stoml3*$^{-/-}$
Aβ-fibres	RAM	Percentage of total	50% (42/84)	49% (18/37)	37% (15/41)	48% (29/60)	43% (30/70)
		CV (m s^{-1})	13.7 ± 2.8	14.1 ± 2.9	15.33 ± 0.9	13.7 ± 3.0	14.6 ± 3.4
		vFT (mN)	0.4 (0.4–1.0)	0.4 (0.4–0.4)	1.0 (0.4–1.0)	0.4 (0.4–0.4)	0.4 (0.4–1.0)
	SAM	Percentage of total	50% (42/84)	51% (19/37)	63% (26/41)	52% (31/60)	57% (40/70)
		CV (m s^{-1})	13.5 ± 2.5	15.4 ± 2.7	16.13 ± 0.7	14.4 ± 3.2	14.7 ± 3.5
		vFT (mN)	1.0 (0.4–1.0)	1.0 (0.4–1.0)	1.4 (0.4–10)	1.0 (0.4–1.0)	1.0 (0.4–2.0)
Aδ-fibres	D-hair	Percentage of total	29% (24/83)	27% (12/44)	30% (8/27)	34% (24/70)	46% (26/56)
		CV (m s^{-1})	5.9 ± 1.9	5.3 ± 0.9	6.2 ± 0.64	5.4 ± 1.5	6.2 ± 1.9
		vFT (mN)	0.4	0.4	0.4	0.4	0.4
	AM	Percentage of total	71% (59/83)	73% (32/44)	70% (19/27)	66% (46/70)	54% (30/56)
		CV (m s^{-1})	6.3 ± 3.0	6.0 ± 2.8	5.88 ± 0.66	6.1 ± 3.4	5.1 ± 3.3
		vFT (mN)	3.3 (2.0–6.3)	6.3 (4.8–10.0)***	6.3 (1.0–22)	4.8 (3.3–6.3)*	10 (6.3–22.4)***
C-fibres	All C	Total number	(82)	(49)	(23)	(54)	(30)
		CV (m s^{-1})	0.48 ± 0.15	0.44 ± 0.11	0.53 ± 0.07	0.45 ± 0.11	0.53 ± 0.11
		vFT (mN)	3.3 (3.3–6.3)	6.3 (3.3–10)*	6.3 (6.3–6.3)	6.3 (6.3–10)***	6.3 (3.3–10)
	C-MH	Percentage of total	64% (35/55)	75% (32/43)	59% (10/17)	57% (21/37)	46% (13/28)
		CV (m s^{-1})	0.42 ± 0.08	0.41 ± 0.10	0.57 ± 0.15	0.40 ± 0.09	0.51 ± 0.12
		vFT (mN)	3.3 (3.3–6.3)	6.3 (6.3–10)***	6.3 (2.0–6.3)	6.3 (6.3–10)***	6.3 (3.3–10)
	C-M	Percentage of total	36% (20/55)	25% (11/43)	41% (10/17)	43% (16/37)	54% (15/28)
		CV (m s^{-1})	0.50 ± 0.16	0.51 ± 0.07	0.49 ± 0.06	0.42 ± 0.09	0.54 ± 0.10
		vFT (mN)	6.3 (3.3–8.2)	6.3 (6.3–8.2)	6.3 (6.3–9.08)	4.8 (3.3–8.2)	3.3 (2.6–6.3)

Electrical search	Controls	*asic3*$^{-/-}$	*stomatin*$^{-/-}$:*stoml3*$^{-/-}$	*asic3*$^{-/-}$:*stomatin*$^{-/-}$	*asic3*$^{-/-}$:*stoml3*$^{-/-}$
Aβ-fibres	5% (4/73)	0% (0/11)	41% (9/22)**	7% (2/27)	27% (10/37)**
Aδ-fibres	8% (3/37)	8% (1/12)	35% (6/17)*	13% (3/24)	26% (7/27)*
C-fibres	8% (4/49)	7% (1/15)	15% (2/13)	8% (2/23)	16% (2/13)

Properties of sensory receptor subtypes in controls, *asic*$^{3-/-}$, *asic*$^{3-/-}$:*stomatin*$^{-/-}$; *stomatin*$^{-/-}$:*stoml3*$^{-/-}$ *and asic3*$^{-/-}$:*stoml3*$^{-/-}$. Conduction velocity and von Frey mechanical threshold in mutant mice were compared to controls using the Mann–Whitney rank sum test. Proportions of mechanically insensitive receptors were compared using Fisher's exact test.*$P < 0.05$, **$P < 0.01$, ***$P < 0.005$.

Table 2 Properties of sensory receptor subtypes in control, *asic2*$^{-/-}$ *and asic2*$^{-/-}$:*stomatin*$^{-/-}$ mutant mice

Mechanical search			Controls	*asic2*$^{-/-}$	*asic2*$^{-/-}$:*stomatin*$^{-/-}$
Aβ-fibres	RAM	Percentage of total	36% (15/42)	42% (36/86)	42% (39/92)
		CV (m s^{-1})	16.9 ± 1.3	18.8 ± 0.9	16.7 ± 0.6
		vFT (mN)	1.0 (0.4–1.4)	1.2 (1.0–3.3)	0.4 (0.4–1.0)
	SAM	Percentage of total	64% (27/42)	48% (50/86)	58% (53/92)
		CV (m s^{-1})	14.9 ± 1.0	18.8 ± 0.9	17.4 ± 0.6
		vFT (mN)	3.3 (1.2–4.8)	2.7 (1.1–6.3)	1.0 (1.0–2.0)
Aδ-fibres	D-hair	Percentage of total	41% (12/29)	29% (18/62)	54% (45/82)
		CV (m s^{-1})	6.1 ± 0.4	5.7 ± 0.4	5.4 ± 0.2
		vFT (mN)	0.4	0.4	0.4
	AM	Percentage of total	59% (17/29)	71% (44/62)	46% (38/82)
		CV (m s^{-1})	4.8 ± 0.5	5.8 ± 0.3	4.9 ± 0.5
		vFT (mN)	3.3 (2.0–6.3)	3.3 (3.3–6.3)	3.3 (3.3–10)
C-fibres	All C	Number	(32)	(15)	(40)
		CV (m s^{-1})	0.52 ± 0.03	0.45 ± 0.03	0.57 ± 0.03
		vFT (mN)	6.3 (3.3–6.3)	3.3 (2.0–5.5)	3.3 (2–6.3)
	CMH	Percentage of total	40% (8/20)	64% (7/11)	63% (12/19)
		CV (m s^{-1})	0.49 ± 0.02	0.40 ± 0.02	0.51 ± 0.04
		vFT (mN)	2.0 (2.0–4.05)	3.3 (2.65–4.8)	3.3 (1.85–4.09)
	CM	Percentage of total	60% (12/20)	36% (4/11)	37% (7/19)
		CV (m s^{-1})	0.52 ± 0.06	0.51 ± 0.06	0.61 ± 0.07
		vFT (mN)	6.3 (3.3–10)	2.7 (1.75–3.3)	3.3 (2.65–4.8)

Electrical search		Controls	*asic2*$^{-/-}$	*asic2*$^{-/-}$:*stomatin*$^{-/-}$
Mechanically insensitive units	Aβ-fibres	4% (1/24)	12% (12/97)	8% (2/24)
	Aδ-fibres	7% (4/57)	5% (3/66)	25% (12/48)
	C-fibres	9% (3/32)	7% (1/15)	18% (7/37)

Properties of sensory receptor subtypes in control, *asic2*$^{-/-}$ and *asic2*$^{-/-}$:*stomatin*$^{-/-}$ mice. Conduction velocity and von Frey mechanical threshold in mutant mice were compared to controls using the Mann–Whitney rank sum test. Proportions of mechanically insensitive receptors were compared using Fisher's exact test.*$P < 0.05$.

physiological properties were specific to this receptor type as we noted no changes in the stimulus–response functions of SAMs recorded from *asic3*$^{-/-}$ and *asic3*$^{-/-}$:*stomatin*$^{-/-}$ mutant mice (Fig. 1*G*). The third major type of low threshold mechanoreceptor found in the skin is the D-hair receptor. The mechanosensitivity of D-hairs was decreased in *asic3*$^{-/-}$:*stomatin*$^{-/-}$ but not in *asic3*$^{-/-}$ mutant mice ($P = 0.068$, repeated measures ANOVA, Fig. 1*H*). This finding is consistent with previously published data that the loss of stomatin alone leads to

a loss of D-hair receptor sensitivity (Martinez-Salgado *et al.* 2007).

Acute blockade of ASIC3 selectively enhances rapidly adapting mechanoreceptor sensitivity

APETx2 is a peptide toxin from the sea anemone (*Anthopleura elegantissima*), and has been shown to selectively inhibit ASIC3-containing ion channels (Diochot *et al.* 2004, 2007). We tested a total of 12 rapidly adapting and 7 slowly adapting mechanoreceptors in six C57BL/6N mice. Ten minutes after the addition of 5 μM APETx2 to the isolated receptive field, the firing rate of RAMs increased significantly while applying a ramp stimulus with a velocity of 450 μm s^{-1}; however, no effect was observed with a faster ramp of velocity 1500 μm s^{-1}

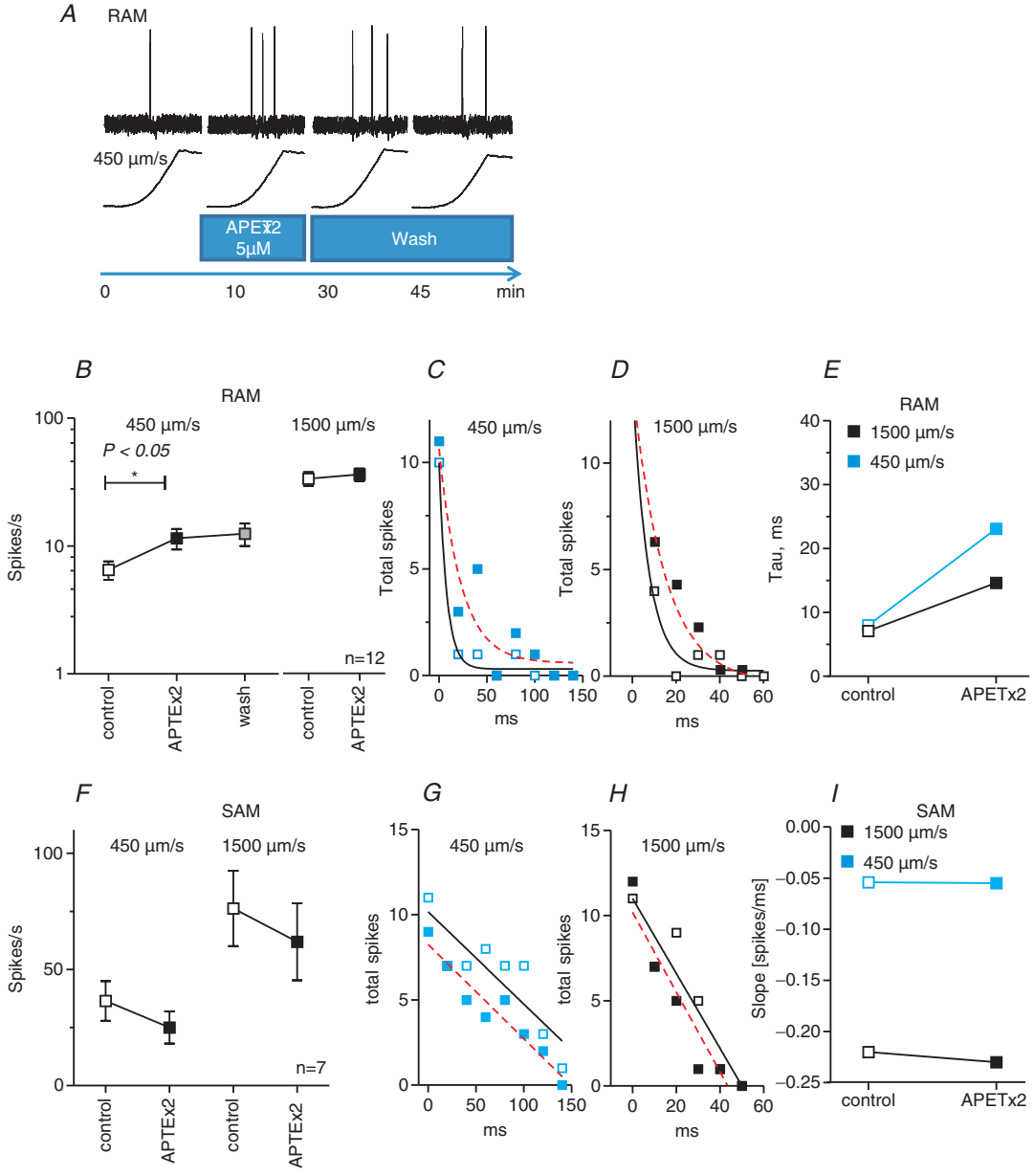

Figure 2. Response properties of rapidly and slowly adapting mechanoreceptors after local APETx2 application
A shows the response of a RAM to APETx2. Note that washout was incomplete after 60 min. Stimulus force traces are shown. '450 μm s^{-1}' refers to the movement velocity of the probe and corresponds to a force of 1.3 mN ms^{-1}. *B*, firing rate increased significantly for RAMs. *C*, *D* and *E* show the cumulative response was fitted to an exponential function. The time constants 'τ' at 1500 and 450 μm s^{-1} were increased under APETx2. In contrast, there was no change in discharge rate for SAM under APETx2 (*F*). *G*, *H* and *I*, the cumulative response for SAM during the ramp phase was fitted with a linear function; comparison shows no change in slopes.

($P = 0.05$, Mann–Whitney test; Fig. 2*B*). The cumulative distribution of spikes in bins of 20 ms for 450 μm s^{-1} and 10 ms for 1500 μm s^{-1} stimulation velocities from all units was fitted to a one-phase exponential decay function in order to calculate the mean decay or adaptation time constant (τ). Under APETx2, τ increased from 8 ms to 23.1 ms (at 450 μm s^{-1}) and from 7.1 ms to 14.6 ms (at 1500 μm s^{-1}) (Fig. 2*C–E*). There was no return to baseline responses after a washout period for up to 60 min. We observed no change in adaptation during the ramp phase in slowly adapting mechanoreceptors exposed to the same concentrations of APETx2 for the same length of time (Fig. 2*F–I*).

Properties of nociceptors in *asic3*$^{-/-}$:*stomatin*$^{-/-}$ double mutant mice

A large sample of C-fibre ($n = 49$) and Aδ-nociceptors ($n = 41$) was studied from *asic3*$^{-/-}$:*stomatin*$^{-/-}$ mice (Fig. 3). In agreement with a previous study, the mechanosensitivity of AMs is significantly attenuated in the absence of ASIC3 ($P < 0.05$, repeated measures ANOVA; Fig. 3*B*). We asked whether the additional loss of stomatin would introduce additional alterations in the AMs in *asic3*$^{-/-}$:*stomatin*$^{-/-}$ mutant mice when compared to controls or *asic3*$^{-/-}$ mice. The stimulus–response properties of AMs in *asic3*$^{-/-}$:*stomatin*$^{-/-}$ double mutants were significantly reduced compared to control ($P < 0.0005$, repeated measures ANOVA with Bonferroni *post hoc* tests; Fig. 3*B*). However, the assessment of the mechanosensitivity of AMs in *asic3*$^{-/-}$:*stomatin*$^{-/-}$ mice indicated no additional effect on AM fibre sensitivity when compared with *asic3*$^{-/-}$ mice ($P > 0.05$, repeated measures ANOVA; Fig. 3*B*). The median von Frey thresholds for the AM mechanonociceptors were significantly elevated in both *asic3*$^{-/-}$ and *asic3*$^{-/-}$:*stomatin*$^{-/-}$ compared to controls, an effect that parallels the changes in the stimulus–response functions. (Table 1, $P < 0.0001$, Mann–Whitney rank sum test). Another measure of mechanical threshold is the minimum mechanical latency which is the time from

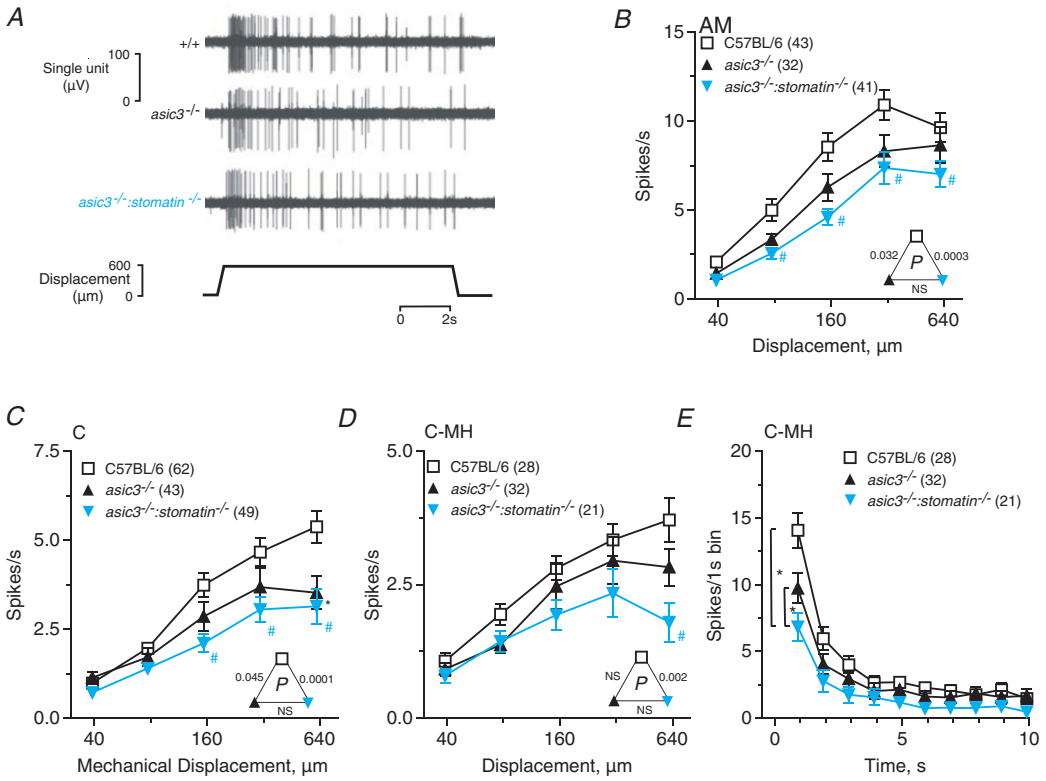

Figure 3. Responses of C- and A-mechanonociceptors in control, *asic3*$^{-/-}$ and *asic3*$^{-/-}$:*stomatin*$^{-/-}$ mice
A, illustration of a representative mechanically evoked discharge from AM in mutant. *B* and *C*, response of AMs and C-fibres in *asic3*$^{-/-}$ and *asic3*$^{-/-}$:*stomatin*$^{-/-}$ mice were significantly reduced compared to control ($P < 0.05$, repeated measures ANOVA). *D*, the decrease in stimulus–response functions was evident in polymodal heat-sensitive C-MHs. *E*, time histogram of C-MHs during 10 s stimulation with 614 μm displacement. The peak firing during the first second was significantly lower in *asic3*$^{-/-}$:*stomatin*$^{-/-}$ compared to *asic3*$^{-/-}$ and control ($P < 0.05$, one-way ANOVA). Error bars indicate SEM. *$P < 0.05$, Bonferroni *post hoc* test *asic3*$^{-/-}$ *vs.* control. #$P < 0.05$, Bonferroni *post hoc* test *asic3*$^{-/-}$:*stomatin*$^{-/-}$ *vs.* control.

the start of the ramp until the first spike corrected for conduction delay (Milenkovic *et al.* 2008). The mean mechanical latencies for AMs in *asic3*$^{-/-}$ (60.9 ± 11 ms) or *asic3*$^{-/-}$:*stomatin*$^{-/-}$ (74 ± 9.8 ms) double mutant mice did not differ significantly from those in controls (53.8 ± 8.9 ms) for a 156 μm stimulus (mean ± SEM; $P > 0.05$, Kruskal–Wallis test).

The largest group of nociceptors has unmyelinated C-fibre axons. The responses of C-fibres to suprathreshold mechanical stimulation was significantly reduced in both *asic3*$^{-/-}$ ($n = 43$) and *asic3*$^{-/-}$:*stomatin*$^{-/-}$ double mutants ($n = 49$) compared to controls ($n = 62$) ($P < 0.05$ for *asic3*$^{-/-}$, $P < 0.0001$ for *asic3*$^{-/-}$:*stomatin*$^{-/-}$, repeated measures ANOVA; Fig. 3*C*). There was no significant difference between the stimulus–response function of C-fibres recorded from *asic3*$^{-/-}$ and *asic3*$^{-/-}$:*stomatin*$^{-/-}$ mutants ($P > 0.05$, repeated measures ANOVA, Fig. 3*C*), indicating that loss of stomatin did not strongly accentuate the moderate loss of C-fibre mechanosensitivity observed in *asic3*$^{-/-}$ mice. The minimum mean mechanical latencies of mutant C nociceptors were not altered in *asic3*$^{-/-}$ (136 ± 15 ms) or *asic3*$^{-/-}$:*stomatin*$^{-/-}$ (143 ± 19 ms) compared to controls (113 ± 14 ms) ($P > 0.05$, Kruskal–Wallis test).

We have observed that the mechanosensitivity of noxious heat-sensitive C-mechanoheat units (C-MHs) is on average significantly less than that of C-mechano fibres (C-Ms) in terms of maximum suprathreshold firing rates (Milenkovic *et al.* 2008). Therefore, we analysed the stimulus–response properties of C-MHs and C-M fibres separately. This analysis revealed that C-MH fibres recorded from *asic3*$^{-/-}$:*stomatin*$^{-/-}$ double mutant mice displayed significantly lower mean firing rates at higher stimulus strengths than control C-MHs ($P < 0.005$, repeated measures ANOVA; Fig. 3*D*). Nevertheless, there was no statistically significant difference between the stimulus–response properties of C-MH fibres measured from *asic3*$^{-/-}$ and *asic3*$^{-/-}$:*stomatin*$^{-/-}$ mutant mice ($P > 0.05$, repeated measures ANOVA; Fig. 3*D*). To resolve this discrepancy, we further analysed the discharge pattern to the strongest stimulus applied (624 μm). C-fibres exhibit prominent adaptation during the course of a 10 s static stimulus (Fig. 3*E*). Post-stimulus time histograms (1 s bins) of the response of each C-MH were fitted to a one-phase exponential decay function ($Y = Ae^{-bx}$), where A and b values describe the peak discharge and adaptation, respectively. The peak firing rate (A) from *asic3*$^{-/-}$:*stomatin*$^{-/-}$ nulls was 6.0 ± 0.6 spikes s^{-1}, from *asic3*$^{-/-}$ nulls 7.9 ± 0.6 spikes s^{-1} and from controls 11.9 ± 0.7 spikes s^{-1}. Taking the A value as an indicator of peak firing, we detected a significant decrease in firing, during the 1st second of the stimulus, in *asic3*$^{-/-}$:*stomatin*$^{-/-}$ C-MHs (6.8 ± 1.0 spikes s^{-1}) compared to *asic3*$^{-/-}$ C-MHs (9.7 ± 1.1 spikes s^{-1}) and to control C-MHs (14.1 ± 1.3 spikes s^{-1}) ($P < 0.0005$, one-way ANOVA with Bonferroni *post hoc* test, Fig. 3*E*). The b values were 1.02 ± 0.14 s for controls, and 1.13 ± 0.23 s for *asic3*$^{-/-}$ and 0.98 ± 0.23 s for *asic3*$^{-/-}$:*stomatin*$^{-/-}$ mutants. In contrast to the results of the C-MH analysis the same analysis of C-M stimulus–response functions in wild-type, *asic3*$^{-/-}$ and *asic3*$^{-/-}$:*stomatin*$^{-/-}$ double mutant mice did not reveal any significant changes in mechanosensitivity.

In summary, we found that the absence of ASIC3 leads to an apparent increase in RAM firing rate. The reason for the increased firing rates in RAMs is a substantial loss of spike adaptation during ramp stimuli in the absence of ASIC3; there appears to be no influence of stomatin in this process. The enhanced sensitivity of RAMs due to reduced adaptation could be mimicked by acute block of ASIC3 at the receptor endings suggesting for the first time that ASIC3 may directly participate in spike encoding. Among nociceptors loss of ASIC3 attenuates the mechanosensitivity of AM and C-MH nociceptors and these effects were sometimes accentuated by the additional loss of stomatin.

Properties of mechanoreceptors and nociceptors in *asic3*$^{-/-}$:*stoml3*$^{-/-}$ mutant mice

STOML3 is the closest mammalian protein to stomatin based on amino acid sequence and deletion of the *stoml3* gene in mice leads to a profound loss of mechanosensitivity in myelinated sensory fibres (Wetzel *et al.* 2007; Lapatsina *et al.* 2012*a*,*b*). However, our initial studies of STOML3 mutant mice indicated that the mechanosensitivity of C-fibre nociceptors was largely unaffected by the deletion of the *stoml3* gene (Wetzel *et al.* 2007). We generated *asic3*$^{-/-}$:*stoml3*$^{-/-}$ mutant mice in order to ask whether the lack of interaction between these two genes leads to additional changes in the physiology of sensory afferents. One of the major findings in *stoml3*$^{-/-}$ mutant mice was that around 35% of the myelinated fibres lack a mechanosensitive receptive field when examined with an electrical search stimulus. We determined the proportion of Aβ-fibres (CV > 10 m s^{-1}) with no mechanosensitive receptive field and found the proportion to be significantly elevated (27%, 10/37 fibres) in *asic3*$^{-/-}$:*stoml3*$^{-/-}$ compared to the proportions found in controls or *asic3*$^{-/-}$ single mutant mice ($P < 0.05$, Fisher's exact test, Fig. 4*A*). The proportion of mechanoinsensitive Aβ-fibres found in the *asic3*$^{-/-}$:*stoml3*$^{-/-}$ double mutant mice was similar to that reported in *stoml3*$^{-/-}$ mutant mice (Wetzel *et al.* 2007), indicating that ASIC3 deficiency does not exacerbate this aspect of the *stoml3*$^{-/-}$ mutant phenotype.

Most of our analyses of single units in *asic3*$^{-/-}$:*stoml3*$^{-/-}$ mutant mice were focused on sensory afferents isolated using a mechanical search

stimulus. We found that the stimulus–response behaviour of Aβ-fibres was essentially the same as has previously been reported for such fibres in *stoml3*$^{-/-}$ single mutants. Thus, among the units classified as RAMs, 39% (13/30 fibres) were classified as so called 'tap' units because they did not respond to the fastest velocity stimulus, and at most one action potential could be elicited with strong tapping stimulus administered with a glass rod (Fig. 4*B*). The remaining RAMs had normal mechanosensitivity and mechanical latencies compared to controls (Fig. 4*C*). We did not note a substantial slowing of adaptation during a ramp stimulus in RAMs from *asic3*$^{-/-}$:*stoml3*$^{-/-}$ mice, as was seen in *asic3*$^{-/-}$ mutant mice (Fig. 1) (data not shown). The mechanosensitivity of D-hair and SAM receptors recorded in *asic3*$^{-/-}$:*stoml3*$^{-/-}$ mutant mice was similar to that of controls (Fig. 4*D* and *E*).

Similar to the *stoml3*$^{-/-}$ mutant mice a large proportion of Aδ-fibres in *asic3*$^{-/-}$:*stoml3*$^{-/-}$ were also mechanoinsensitive as shown using the electrical search technique (Fig. 4*A*). We made a detailed study of mechanosensitive Aδ-fibres that could be classified as mechanonociceptors (AMs). We first noted a substantial increase in the median von Frey threshold of AMs measured in *asic3*$^{-/-}$:*stoml3*$^{-/-}$ double mutants which was significantly different from median von Frey thresholds found for control AM fibres and AM fibres recorded from *asic3*$^{-/-}$ single mutants (control $P < 0.0001$, *asic3*$^{-/-}$ $P < 0.05$, Mann–Whitney rank sum test). The extremely high mechanical threshold of AMs recorded from *asic3*$^{-/-}$:*stoml3*$^{-/-}$ was also reflected in a substantial flattening of the stimulus–response function of AMs to suprathreshold stimuli (Fig. 5*B*). Thus the mean maximum firing rates of AMs recorded from *asic3*$^{-/-}$:*stoml3*$^{-/-}$ mutant mice were less than 50% of those in controls. The stimulus–response function of AMs recorded from *asic3*$^{-/-}$:*stoml3*$^{-/-}$ mutant mice differed significantly from controls and also compared to *asic3*$^{-/-}$ mutant mice (control $P < 0.0001$, *asic3*$^{-/-}$ $P < 0.005$, repeated measures ANOVA; Fig. 5*B*).

C-fibres recorded from *asic3*$^{-/-}$:*stoml3*$^{-/-}$ double mutants had mechanical thresholds that did not differ from those found for C-fibres in control mice (Table 1). In parallel, the C-fibre mechanosensitivity in *asic3*$^{-/-}$:*stoml3*$^{-/-}$ mutant mice was unaltered compared to controls ($P > 0.05$, repeated measures ANOVA; Fig. 5*C*). The stimulus–response functions of C-MH units from *asic3*$^{-/-}$:*stoml3*$^{-/-}$ mutant mice were unaltered compared to control and *asic3*$^{-/-}$ mutants ($P > 0.05$, repeated measures ANOVA; Fig. 5*D*).

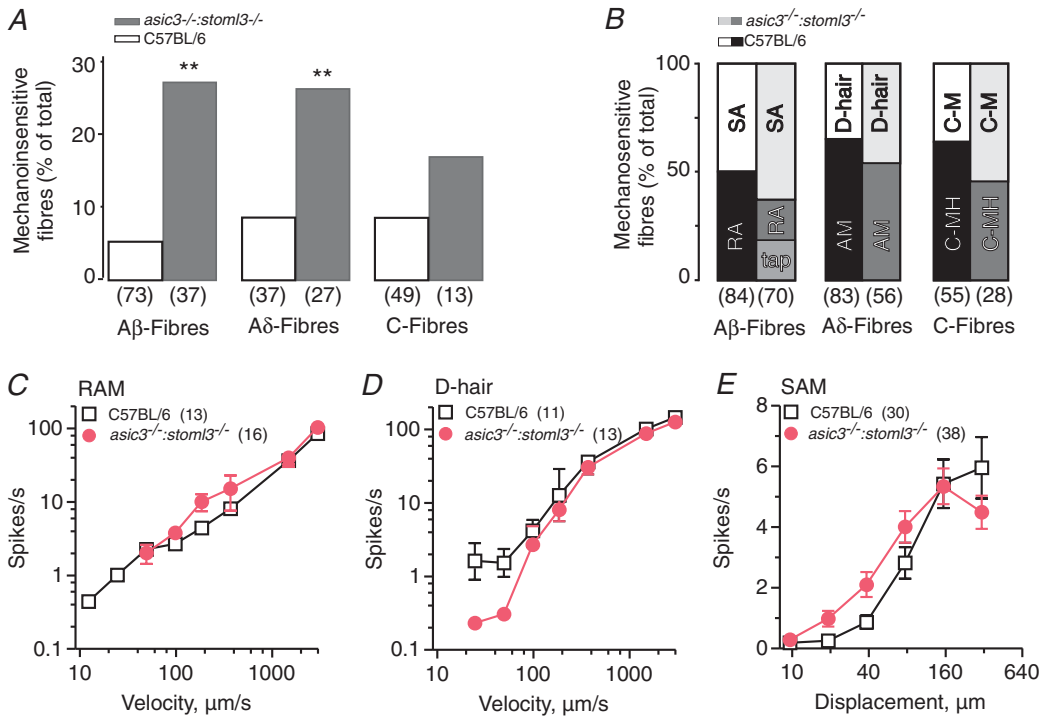

Figure 4. Mechanically insensitive and low threshold receptors in *asic3*$^{-/-}$:*stoml3*$^{-/-}$
A, in *asic3*$^{-/-}$:*stoml3*$^{-/-}$ mice a larger proportion of A-fibre sensory afferents were mechanically insensitive whereas C-fibres were not affected (*$P < 0.01$ and **$P < 0.001$, Fisher's exact test). *B*, proportions of mechanically sensitive receptor subtypes were not changed among Aβ-, Aδ- and C-fibres, but note an increase in RAM 'tap' units. *C*, response properties of RAM and D-hairs were not altered in *asic3*$^{-/-}$:*stoml3*$^{-/-}$ mice. *C–E*, the remaining RAM units, SAM and D-hairs had normal mechanosensitivity. Error bars indicate SEM.

Properties of mechanoreceptors and nociceptors in *asic2*$^{-/-}$:*stomatin*$^{-/-}$ mutant mice

Heterologous expression of stomatin with ASIC2 channels has been reported to modulate the inactivation kinetics of proton-gated currents carried by these channels (Price *et al.* 2004; Lapatsina *et al.* 2012*a*). It was reported that RAMs show an impairment in mechanosensitivity in *asic2*$^{-/-}$ mice (Price *et al.* 2000), although similar effects were not reported in another *asic2* mutant mouse (Roza *et al.* 2004). We generated *asic2*$^{-/-}$:*stomatin*$^{-/-}$ mutant mice to ask whether the absence of stomatin might accentuate phenotypes found in *asic2*$^{-/-}$ mice. The *asic2*$^{-/-}$ allele generated ensured that both ASIC2a and ASIC2b isoforms were absent (Price *et al.* 2000). In this set of experiments data from *asic2*$^{-/-}$:*stomatin*$^{-/-}$ and *asic2*$^{-/-}$ mutants were compared with data from *asic2*$^{+/+}$:*stomatin*$^{+/+}$ mice which were obtained from inter-crosses and were on a mixed genetic background (Milenkovic *et al.* 2008). We used the electrical search technique to ask whether a substantial number of fibres lacked mechanosensitivity in any of the genotypes. Electrical search data from comparing *asic*$^{+/+}$:*stomatin*$^{-/-}$ mice and *asic2*$^{+/+}$:*stomatin*$^{+/+}$ wild-type mice has been published (Martinez-Salgado *et al.* 2007) and indicated that stomatin loss does not lead to an increase in the incidence of mechanoinsensitive fibres. All experiments were carried out blind to the genotype and the results were as follows: amongst Aβ-fibres there was no increase in mechanically insensitive fibres in any of the genotypes studied, including *asic2*$^{-/-}$:*stomatin*$^{+/+}$ and *asic2*$^{-/-}$:*stomatin*$^{-/-}$ mice. This situation was substantially different amongst Aδ-fibres as here we found that a substantial proportion, 25% (12/48 fibres), of these fibres were mechanically insensitive compared to just 4% (1/24 fibres) for *asic2*$^{+/+}$:*stomatin*$^{+/+}$ control mice and other control genotypes, e.g. in C57BL/6N mice, 5% (4/73 fibres) (see Table 1). Thus around a quarter of Aδ-fibres are mechanically insensitive

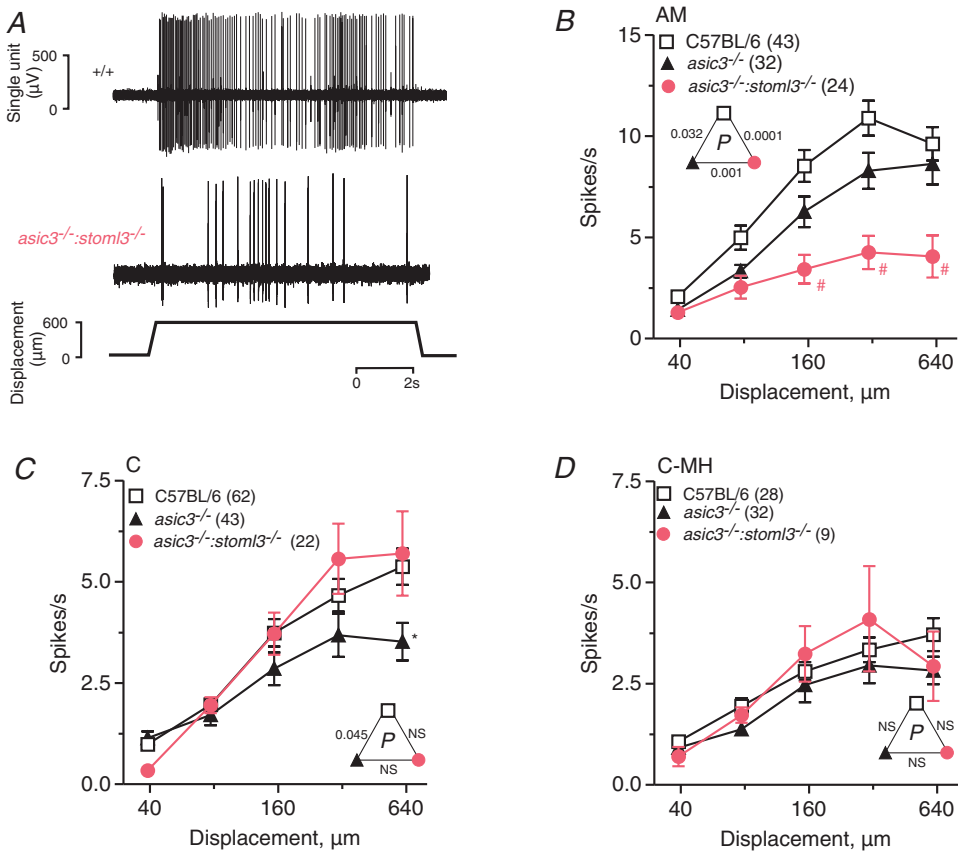

Figure 5. Responses of C- and Aδ- mechanonociceptors in *asic3*$^{-/-}$:*stoml3*$^{-/-}$ mice
A, illustration of a representative mechanically evoked discharge from AM from control and *asic3*$^{-/-}$:*stoml3*$^{-/-}$ mice. *B*, the stimulus–responses of AMs were dramatically impaired in *asic3*$^{-/-}$:*stoml3*$^{-/-}$ mutant mice compared to controls and *asic3*$^{-/-}$ mice ($P < 0.05$, repeated measures ANOVA with Bonferroni *post hoc* test). *C*, the stimulus–response curve of *asic3*$^{-/-}$:*stoml3*$^{-/-}$ C-fibres was normal and did not match that of *asic3*$^{-/-}$ single mutants. *D*, analysis of C-MH stimulus–response curves was not different in *asic3*$^{-/-}$:*stoml3*$^{-/-}$ compared to controls and *asic3*$^{-/-}$. Error bars indicate SEM. *$P < 0.05$, Bonferroni *post hoc* test *asic3*$^{-/-}$ *vs.* control. #$P < 0.05$, Bonferroni *post hoc* test *asic3*$^{-/-}$:*stoml3*$^{-/-}$ *vs.* control.

in *asic2*$^{-/-}$:*stomatin*$^{-/-}$ mice and this difference was statistically significant (Fisher's exact test $P < 0.01$, Fig. 6*A*). Aδ-fibres can give rise either to AMs which are nociceptors or D-hair receptors which are ultra-sensitive mechanoreceptors. The electrical search experiment does not tell us whether only AMs or only D-hair receptors or both D-hair receptors and AMs become mechanically insensitive. We thus carried out additional blind experiments where a mechanical search stimulus was used to find and identify both Aδ- and Aβ-fibres. Using this technique the proportion of receptor types found is very stereotypical (Lewin, 1996) and we reasoned that if only one receptor type selectively loses mechanosensitivity in *asic2*$^{-/-}$:*stomatin*$^{-/-}$ then one would tend to over-sample the unaffected receptor type. Such an effect was not found for Aβ-fibres where the proportion of fibres classified as RAM or SAM was found not to be different between measurements made in C57BL/6N, *asic2*$^{+/+}$:*stomatin*$^{+/+}$ and *asic2*$^{-/-}$:*stomatin*$^{-/-}$ mice (Fig. 6*B* and Table 2). In contrast, among Aδ-fibres we sampled more D-hair receptors (∼54%) with the mechanical search technique than we did in control mice (∼41%). This shift in the sampled population was statistically significant (Fisher's exact test $P < 0.01$) and is consistent with the idea that AMs are under-sampled because many are not activated at all by the mechanical search stimuli used. We also gathered data on the percentage of C-fibres that apparently lacked mechanosensitivity but there was no statistically significant increase in the percentage of mechanically insensitive C-fibres in any of the genotypes studied (Fig. 6*A*); there was also no significant shift in the proportion of C-fibres classified as C-MH or C-M (Table 2). Nevertheless, the percentage of mechanically insensitive C-fibres in *asic2*$^{-/-}$:*stomatin*$^{-/-}$ appeared quite high (19%, 7/37 fibres tested) compared to controls; $P < 0.1$, Fisher's exact test (see Fig. 6*A* and Table 2). In these sets of experiments the mechano-sensitivity of mechanoreceptors and nociceptors was

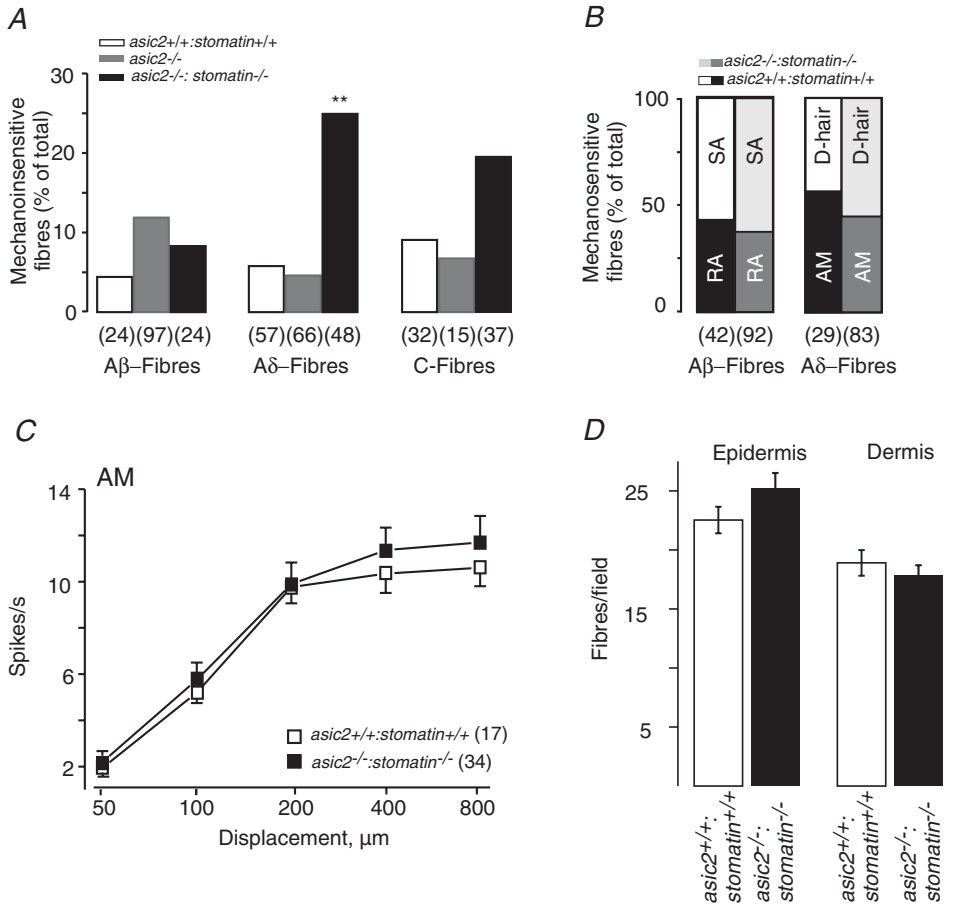

Figure 6. Mechanically insensitive Aδ-mechanonociceptors in *asic2*$^{-/-}$:*stomatin*$^{-/-}$ mice
A, in *asic2*$^{-/-}$:*stomatin*$^{-/-}$ mice a larger proportion of Aδ-nociceptors was mechanically insensitive (*$P < 0.05$, Fisher's exact test). *B*, proportions of mechanically sensitive receptor subtypes were consequently altered among Aδ-fibres. *C*, the stimulus–response function of mechanosensitive AMs was not altered in *asic2*$^{-/-}$:*stomatin*$^{-/-}$ mice. *D*, mean number of individual myelinated and unmyelinated axons counted in epidermis and dermis under 20-fold magnification in microscopic field. Error bars indicate SEM.

examined using a manually applied stimulus (Price *et al.* 2000; Martinez-Salgado *et al.* 2007), thus the speed and displacement amplitude was not precisely controlled. Nevertheless, the stimulus–response functions indicated that the mechanosensitivity of RAMs in this new set of experiments from *asic2*$^{-/-}$:*stomatin*$^{+/+}$ and *asic2*$^{-/-}$:*stomatin*$^{-/-}$ was impaired to the same extent as reported previously. There was, however, no indication that mechanoreceptor function in *asic2*$^{-/-}$:*stomatin*$^{-/-}$ mice was impaired to any greater extent than in *asic2*$^{-/-}$:*stomatin*$^{+/+}$ mice (data not shown). Nociceptors are primarily sensitive to static displacement, thus the manual application of displacement stimuli can more readily be compared with stimuli applied with a computer-controlled stimulator. Despite the fact that a large proportion of AM fibres lacked mechanosensitivity in *asic2*$^{-/-}$:*stomatin*$^{-/-}$ we found that the mechanosensitivity of the remaining AMs was not different from AMs in control *asic2*$^{+/+}$:*stomatin*$^{+/+}$ mice (Fig. 6*C*). These data were also supported by the fact that median von Frey thresholds of AMs in both these genotypes were also not elevated (Table 2).

We also carried out experiments to examine the anatomical integrity of sensory neurons and their endings in the skin of *asic2*$^{-/-}$:*stomatin*$^{-/-}$ mutant mice. First, we prepared semi-thin plastic transverse sections of the saphenous nerve from control and *asic2*$^{-/-}$:*stomatin*$^{-/-}$ mutant and counted myelinated axons with a light microscope as described previously (Carroll *et al.* 1998; Stucky *et al.* 2002). We found no difference in the total number of myelinated axons present in the saphenous nerve of double mutant compared to control wild-type (*asic2*$^{-/-}$:*stomatin*$^{-/-}$, 468 ± 13; compared to 481 ± 18 in *asic2*$^{+/+}$:*stomatin*$^{+/+}$, $P > 0.6$, unpaired t test, $n = 4$–6 per group). Thus the lack of mechanosensitivity exhibited by a subpopulation of sensory afferents does not appear to be due to a dying back of sensory axons. To address this issue more directly we removed skin from the saphenous innervation territory of wild-type and *asic2*$^{-/-}$:*stomatin*$^{-/-}$ mutant mice and performed immunofluorescence staining for the pan neuronal marker PGP 9.5. We then made a semi-quantitative analysis of the density of PGP 9.5-positive sensory fibres in the epidermis and dermis of the skin (three experiments per genotype, ~20 sections examined per mouse). The epidermis is predominantly innervated by nociceptive sensory afferents, in particular by myelinated nociceptive afferents (AM fibres; Kruger *et al.* 1981). We found no qualitative difference in the morphology of sensory endings stained for the PGP 9.5 antigen between the two genotypes. More importantly we found no difference in the density of epidermal or dermal PGP 9.5-positive fibres in *asic2*$^{-/-}$:*stomatin*$^{-/-}$ mutants compared to controls (Fig. 6*D*). Together these data suggest that a specific subpopulation of thin myelinated nociceptive sensory afferents form normal endings in the skin of *asic2*$^{-/-}$:*stomatin*$^{-/-}$ mice but nevertheless show no mechanosensitivity.

Properties of mechanoreceptors and nociceptors in *stomatin*$^{-/-}$:*stoml3*$^{-/-}$ mutant mice

Stomatin and STOML3 proteins can interact with each other and are present in the same vesicular compartment (Lapatsina *et al.* 2012*b*; Brand *et al.* 2012). It is thus in principle possible that changes in the mechanosensitivity of afferents in *asic3*$^{-/-}$:*stomatin*$^{-/-}$, *asic3*$^{-/-}$:*stoml3*$^{-/-}$, or *asic2*$^{-/-}$:*stomatin*$^{-/-}$ mutant mice may reflect loss of a stomatin–STOML3 interaction in these mice. We therefore generated *stomatin*$^{-/-}$:*stoml3*$^{-/-}$ mice and characterized their mechanosensory phenotype. Again, a similar and substantial proportion of electrically identified Aβ- (41%) and Aδ- (35%) fibres lacked mechanoreceptive fields (Fig. 7*A* and *B*). The stimulus–response functions of mechanoreceptors such as RAMs, SAMs and D-hair receptors indicated no substantial alteration in mechanosensitivity in these receptors beyond what was observed in *stomatin* or *stoml3* single mutants (Fig. 7*C*–*E*). Nociceptors were also analysed in detail using graded mechanical stimulation and here, too, no major changes in stimulus–response functions or mechanical latency (data not shown) were observed in AMs, C-Ms or C-MH fibres (Fig. 7*F*–*H*).

Peripheral nerve anatomy in *asic3*$^{-/-}$:*stoml3*$^{-/-}$ and *stomatin*$^{-/-}$:*stoml3*$^{-/-}$ mutant mice

Changes in the mechanosensitivity of primary afferents could in principle be a consequence of loss of neighbouring axons from peripheral nerves. Previous work on single *stoml3*$^{-/-}$ mutants has shown that there are no detectable anatomical alterations in the peripheral nerves in the absence of STOML3. Using transmission electron microscopy (St John Smith *et al.* 2012) we examined myelinated and unmyelinated axons in the saphenous nerves of *asic3*$^{-/-}$:*stoml3*$^{-/-}$ and *stomatin*$^{-/-}$:*stoml3*$^{-/-}$ mice and observed no alteration in the number or fine anatomy of these axons (Fig. 8). The absolute number of myelinated axons measured from electronmicrographs is larger than that obtained from light microscopy measurements made here for *asic2*$^{-/-}$:*stomatin*$^{-/-}$ mutants, a fact that reflects the greater resolution of the electron microscope. Nevertheless, in each case appropriate controls were used for comparisons.

Discussion

The acid-sensing ion channels ASIC3 and ASIC2 are required for normal sensory neuron mechanosensitivity and can be modulated by stomatin-domain proteins.

Members of the Deg/ENaC family ASIC3 and ASIC2 probably participate in trimeric complexes with other family members (Jasti *et al.* 2007). Here we generated and characterized four new double mutant mouse models and asked whether the loss of stomatin-domain protein interactions that are involved in ASIC modulation can affect mechanosensory phenotypes observed in *asic* mutant mice. We show that the apparent enhanced mechanosensitivity of RAMs in *asic3*$^{-/-}$ mutant mice is due to a loss of adaptation during skin movement; this phenotype was not influenced by the loss of stomatin or STOML3. Strikingly, by using a local application of toxin that blocks ASIC3-containing channels, we could mimic the effect of genetic deletion of the channel on enhancing mechanosensitivity in RAMs. In contrast, Aδ-mechanonociceptors (AMs) in *asic3*$^{-/-}$ mutant mice were less sensitive to mechanical stimuli and this insensitivity was moderately accentuated by the absence of stomatin and substantially altered by the absence of STOML3 (Figs 3 and 5). Similarly, the interaction between ASIC2 and stomatin was found to be particularly important for AM mechanosensitivity as a quarter of these fibres were found to be mechanically

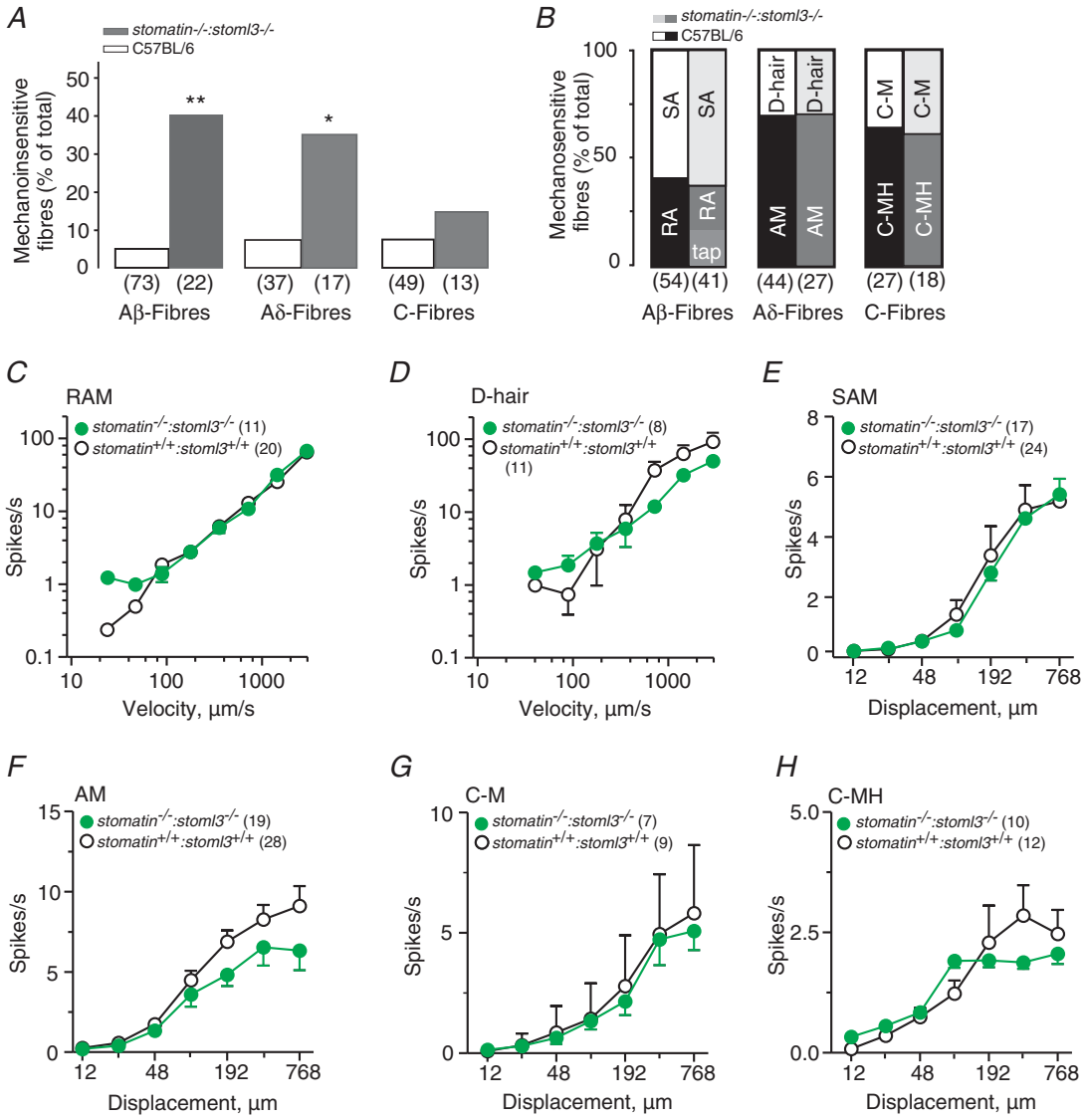

Figure 7. Mechanically insensitive sensory afferents in *stomatin*$^{-/-}$:*stoml3*$^{-/-}$ mice
A, in *stomatin*$^{-/-}$:*stoml3*$^{-/-}$ mice an increased proportion of mechanoinsensitive afferents was found for A-fibres (Fisher's exact test, $^{**}P < 0.005$, $^{*}P < 0.05$) but not for C-fibres ($P > 0.05$) when compared to wild-type littermates. *B*, the proportion of mechanoreceptor subtypes was not changed in *stomatin*$^{-/-}$:*stoml3*$^{-/-}$ mice (χ^2 test $P > 0.05$) compared to controls. *C* and *D*, velocity–response function for RAM and D-hairs revealed no changes in firing frequencies in *stomatin*$^{-/-}$:*stoml3*$^{-/-}$ mice compared to wild-type littermates ($P > 0.05$, repeated measures ANOVA). *E–H*, stimulus–response plots for SAM, AM, C-M and C-MH fibres were not altered in *stomatin*$^{-/-}$:*stoml3*$^{-/-}$ mice. Error bars indicate SEM.

silent in *asic2*$^{-/-}$:*stomatin*$^{-/-}$ mutants (Fig. 6). In contrast to *asic3* single and double mutants we have never found any evidence for effects of *asic2* or *stomatin* single gene deletion on AM mechanosensitivity (Price *et al.* 2000; Martinez-Salgado *et al.* 2007).

In *asic3*$^{-/-}$ mutant mice, C-MH fibres fired less to very intense mechanical stimuli. This decreased sensitivity was enhanced in the additional absence of stomatin and was most prominent at the onset of the stimulus (Fig. 3*E*). Examination of all types of cutaneous afferents in *stomatin*$^{-/-}$:*stoml3*$^{-/-}$ mutants did not reveal any enhancement of phenotypes already present in *stomatin*$^{-/-}$ *or stoml3*$^{-/-}$ mice. Thus, although these proteins are highly related and interact with each other, their sensory functions appear to be independent. See Fig. 9 for a summary of all the phenotypes observed.

Increased mechanosensitivity of cutaneous afferents has been described in *asic3* mutant mice as well as in *asic1a*:*asic2*:*asic3* triple mutant mice (Price *et al.* 2001; Kang *et al.* 2012). Differential effects on the mechanosensitivity of subpopulations of visceral afferents have also been reported after deletion of individual ASICs (Page *et al.* 2005). We show here that deletion of ASIC3 leads to a highly specific enhancement of mechanoreceptor sensitivity in RAMs (Fig. 1). We used precisely controlled ramp-and-hold stimuli to characterize the velocity sensitivity of RAMs which are normally finely tuned to a stereotypical range of frequencies (Johnson, 2001; Heidenreich *et al.* 2012; Lechner & Lewin, 2013). RAMs recorded from *asic3*$^{-/-}$ and *asic3*$^{-/-}$:*stomatin*$^{-/-}$ showed a very substantial increase in firing rates to all velocities tested (Fig. 1). The increased sensitivity was entirely due to reduced adaptation during the ramp movement. Normally, wild-type RAMs adapt substantially during the ramp phase of the stimulus with fast time constants of decay (ranging from 100 to 10 ms). We observed that the speed of adaptation substantially increased as stimulus velocity increased, a property often seen in sensory coding (Eatock, 2000). In the absence of ASIC3, adaptation was slowed by around 10-fold (>1 s) but still adaptation increased in speed with increasing stimulus velocity (Fig. 1).

How does the absence of ASIC3 change adaptation so specifically in RAMs? This finding suggests that

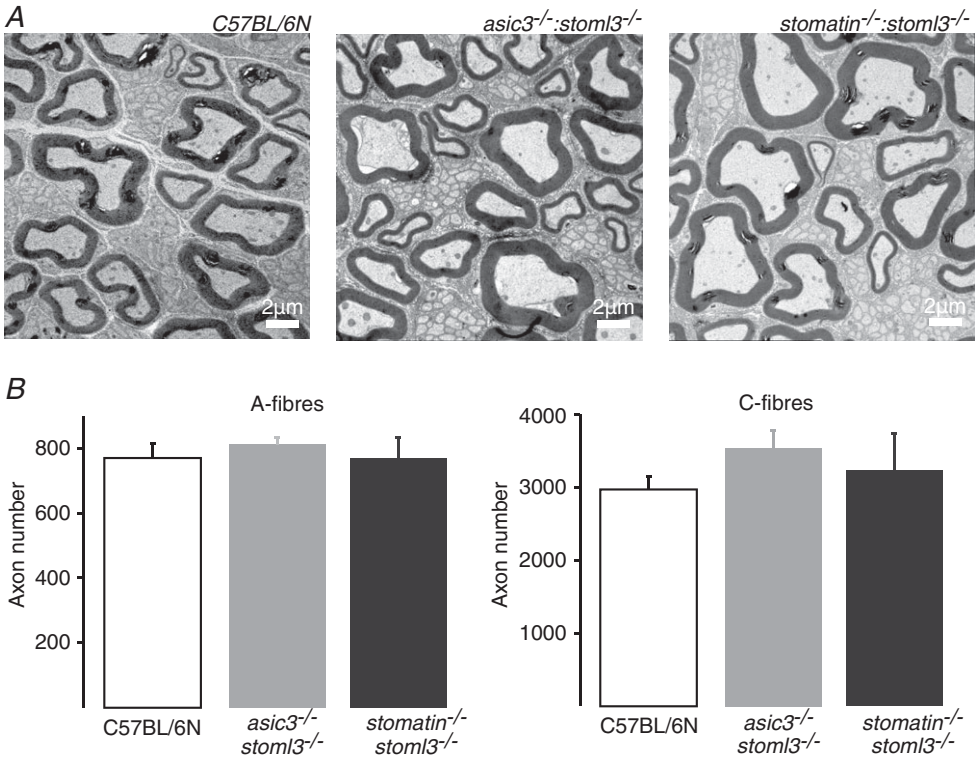

Figure 8. Electron microscopy of the saphenous nerve in double mutant mice
A, examples for a typical electron micrograph of the saphenous nerve (transverse section) of C57BL/6N, *asic3*$^{-/-}$:*stoml3*$^{-/-}$ and *stomatin*$^{-/-}$:*stoml3*$^{-/-}$ mice are shown. Scale bar is 2 μm. *B*, myelinated (A-fibres) and non-myelinated (C-fibres) axons were counted for a representative area of the nerve and extrapolated to the nerve cross-section to determine the total number of axons in each nerve. There was no difference in the total number of axons noted between the genotypes either for A- or for C-fibres ($P > 0.05$, unpaired *t* test). Error bars indicate SEM.

ASIC3 is especially enriched in RAMs but it is also possible that the absence of ASIC3 leads indirectly to the development of this phenotype. However, our finding that the ASIC3-specific toxin APETx2 (Diochot *et al.* 2004, 2007) acutely increased the discharge rate of wild-type RAMs suggests that ASIC3 channels in RAMs directly modulate receptor adaptation. Thus the adaptation during the ramp was substantially slower in the presence of APETx2. However, when we applied the APETx2 to the receptive fields of SAMs, which do not have altered physiological properties in *asic3*$^{-/-}$ mutant mice, there was no effect. This is important as at high doses the APETx2 toxin can have inhibitory effects on voltage-gated K^+ and Na^+ channels (Blanchard *et al.* 2012). Thus the lack of effect of APETx2 on SAMs suggests that ASIC3 channels play no role at the receptor endings of these neurons. ASIC3 in the receptor terminals of RAMs is thus required for fast spike adaptation in a specific mechanoreceptor. It has been shown very recently that RAM development is critically dependent on the transcription factor c-Maf and one consequence of c-Maf loss of function is hypersensitivity of RAMs (Bourane *et al.* 2009; Luo *et al.* 2009). Indeed, RAMs in c-Maf mutant mice also show a marked lack of adaptation similar to that observed here (Wende *et al.* 2012). Another ion channel that has a specific role in tuning RAM receptor sensitivity is KCNQ4 (Heidenreich *et al.* 2012), the transcription of which in mechanoreceptors is under the control of c-Maf (Wende *et al.* 2012). It is thus quite possible that transcription from the *asic3* gene locus may be under the control of c-Maf. Our results clearly show that the additional absence of stomatin in RAMs had no discernible effect on adaptation. However, it is interesting to note that the enhanced sensitivity of RAMs was absent in *asic3*$^{-/-}$:*stoml3*$^{-/-}$ mutant mice (Fig. 4*C*).

Here we noted consistent but moderate impairments in the ability of Aδ-fibre mechanonociceptors (AMs) and C-fibres to maintain high rates of firing to suprathreshold mechanical stimuli in *asic3*$^{-/-}$ mutant mice. Interestingly, the additional loss of stomatin moderately accentuated this phenotype in AMs and in C-MH fibres. The reduced mechanosensitivity of AMs was much more dramatically accentuated by the additional loss of STOML3. Thus, in *asic3*$^{-/-}$:*stoml3*$^{-/-}$ mutant mice, AMs sustained firing rates that were more than 3-fold lower than those found in wild-type mice. Examination of sensory afferent properties in *stomatin*$^{-/-}$:*stoml3*$^{-/-}$ mutant mice suggested that these two genes work independently of each other in regulating mechanosensitivity. It thus appears unlikely that the accentuated mechanosensory phenotypes observed in *asic3*$^{-/-}$:*stoml3*$^{-/-}$, *asic3*$^{-/-}$:*stomatin*$^{-/-}$ *or asic2*$^{-/-}$:*stomatin*$^{-/-}$ are due to the loss of stomatin–STOML3 interactions. The reduced activation of AMs observed in *asic3*$^{-/-}$ mutants is consistent with the observation that pressure-induced vasodilatation in the skin is attenuated in *asic3*$^{-/-}$ mutant mice (Fromy *et al.* 2012), especially considering that AMs contribute directly to vasodilatation (Lewin *et al.* 1992). Our results contrast with those from Kang and colleagues

Receptor type	Genotype							
	asic3$^{-/-}$	*asic2*$^{-/-}$	*stomatin*$^{-/-}$	*asic2*$^{-/-}$:*stomatin*$^{-/-}$	*asic3*$^{-/-}$:*stomatin*$^{-/-}$	*stoml3*$^{-/-}$	*asic3*$^{-/-}$:*stoml3*$^{-/-}$	*stomatin*$^{-/-}$:*stoml3*$^{-/-}$
RAM	↑↑ sensitivity ↓↓ adaptation	↓ sensitivity	No change	Not studied	↑↑ sensitivity ↓↓ adaptation	~35% Mechanically silent	~35% Mechanically silent	~35% Mechanically silent
SAM	No change	No change-	No change	No change	No change	~35% Mechanically silent	~35% Mechanically silent	~35% Mechanically silent
D-hair	No change	No change	↓ sensitivity	↓ sensitivity	↓ sensitivity	~35% Mechanically silent	~35% Mechanically silent	~35% Mechanically silent
AM	↓ sensitivity	No change	No change	~25% Mechanically Silent	↓ sensitivity	~35% Mechanically silent	~35% Mechanically Silent ↓↓ sensitivity	~35% Mechanically silent
C-M	No change	Not studied	No change	No change	No change	No change	No change	No change
C-MH	↓ sensitivity	Not studied	No change	No change	↓↓ sensitivity	No change	↓ sensitivity	No change

Figure 9. Summary of mechanosensory phenotypes in double mutant mice
Summary table of phenotypes per receptor type found in the present study. Light shaded boxes indicate new conclusion made from data obtained in the present study. Non-shaded boxes indicate the conclusions from previous studies, in particular for *asic2*$^{-/-}$ mice (Price *et al.* 2000), *stomatin*$^{-/-}$ mice (Martinez-Salgado *et al.* 2007) and *stoml3*$^{-/-}$ mice (Wetzel *et al.* 2007). The darker shaded boxes indicate cases where the phenotype observed for the receptor type differs significantly from the sum of the phenotypes found in each of the two single mutants.

who observed enhanced mechanosensitivity of AMs in *asic1a*:*asic2*:*asic3* triple mutant mice (Kang *et al.* 2012). The deletion of the *asic1a* and *asic2* genes alone has not been reported to induce changes in the mechanosensitivity of cutaneous AMs (Price *et al.* 2000; Page *et al.* 2004) and so it appears that there may be an unusual interaction between ASIC3 and ASIC1a/ASIC2 regulating nociceptor mechanosensitivity.

In summary, we have shown a new role for ASIC3 in the regulation of RAM adaptation which is independent of stomatin-domain proteins. We have also shown that the genetic deletion of two stomatin-domain proteins, STOML3 or stomatin, accentuate mechanosensitivity deficits found in nociceptive sensory afferents innervating the skin of mice lacking ASIC3 and ASIC2. Thus the regulation of ASIC3 and ASIC2 channels by stomatin-domain proteins has measurable effects on the mechanosensitivity of nociceptors. It is possible that the tuning down of nociceptor mechanosensitivity might be exploited by pharmacological agents that interfere with stomatin-domain protein–ASIC interactions.

References

Arnadóttir J & Chalfie M (2010). Eukaryotic mechanosensitive channels. *Annu Rev Biophys* **39**, 111–137.

Benson CJ, Xie J, Wemmie JA, Price MP, Henss JM, Welsh MJ & Snyder PM (2002). Heteromultimers of DEG/ENaC subunits form H^+-gated channels in mouse sensory neurons. *Proc Natl Acad Sci U S A* **99**, 2338–2343.

Blanchard MG, Rash LD & Kellenberger S (2012). Inhibition of voltage-gated Na^+ currents in sensory neurones by the sea anemone toxin APETx2. *Br J Pharmacol* **165**, 2167–2177.

Bourane S, Garces A, Venteo S, Pattyn A, Hubert T, Fichard A, Puech S, Boukhaddaoui H, Baudet C, Takahashi S, Valmier J & Carroll P (2009). Low-threshold mechanoreceptor subtypes selectively express MafA and are specified by Ret signalling. *Neuron* **64**, 857–870.

Brand J, Smith ESJ, Schwefel D, Lapatsina L, Poole K, Omerbašić D, Kozlenkov A, Behlke J, Lewin GR & Daumke O (2012). A stomatin dimer modulates the activity of acid-sensing ion channels. *EMBO J* **31**, 3635–3646.

Carroll P, Lewin GR, Koltzenburg M, Toyka KV & Thoenen H (1998). A role for BDNF in mechanosensation. *Nat Neurosci* **1**, 42–46.

Chen C-C, Zimmer A, Sun W-H, Hall J, Brownstein MJ & Zimmer A (2002). A role for ASIC3 in the modulation of high-intensity pain stimuli. *Proc Natl Acad Sci U S A* **99**, 8992–8997.

Diochot S, Baron A, Rash LD, Deval E, Escoubas P, Scarzello S, Salinas M & Lazdunski M (2004). A new sea anemone peptide, APETx2, inhibits ASIC3, a major acid-sensitive channel in sensory neurons. *EMBO J* **23**, 1516–1525.

Diochot S, Salinas M, Baron A, Escoubas P & Lazdunski M (2007). Peptides inhibitors of acid-sensing ion channels. *Toxicon* **49**, 271–284.

Drew LJ, Rohrer DK, Price MP, Blaver KE, Cockayne DA, Cesare P & Wood JN (2004). Acid-sensing ion channels ASIC2 and ASIC3 do not contribute to mechanically activated currents in mammalian sensory neurones. *J Physiol* **556**, 691–710.

Driscoll M & Chalfie M (1991). The *mec-4* gene is a member of a family of *Caenorhabditis elegans* genes that can mutate to induce neuronal degeneration. *Nature* **349**, 588–593.

Eatock RA (2000). Adaptation in hair cells. *Annu Rev Neurosci* **23**, 285–314.

Fromy B, Lingueglia E, Sigaudo-Roussel D, Saumet JL & Lazdunski M (2012). Asic3 is a neuronal mechanosensor for pressure-induced vasodilation that protects against pressure ulcers. *Nat Med* **18**, 1205–1207.

Geffeney SL, Cueva JG, Glauser DA, Doll JC, Lee TH-C, Montoya M, Karania S, Garakani AM, Pruitt BL & Goodman MB (2011). DEG/ENaC but not TRP channels are the major mechanoelectrical transduction channels in a *C. elegans* nociceptor. *Neuron* **71**, 845–857.

Geffeney SL & Goodman MB (2012). How we feel: ion channel partnerships that detect mechanical inputs and give rise to touch and pain perception. *Neuron* **74**, 609–619.

Goodman MB, Ernstrom GG, Chelur DS, O'Hagan R, Yao CA & Chalfie M (2002). MEC-2 regulates *C. elegans* DEG/ENaC channels needed for mechanosensation. *Nature* **415**, 1039–1042.

Heidenreich M, Lechner SG, Vardanyan V, Wetzel C, Cremers CW, De Leenheer EM, Aránguez G, Moreno-Pelayo MÁ, Jentsch TJ & Lewin GR (2012). KCNQ4 K^+ channels tune mechanoreceptors for normal touch sensation in mouse and man. *Nat Neurosci* **15**, 138–145.

Huang M, Gu G, Ferguson EL & Chalfie M (1995). A stomatin-like protein necessary for mechanosensation in *C. elegans*. *Nature* **378**, 292–295.

Jasti J, Furukawa H, Gonzales EB & Gouaux E (2007). Structure of acid-sensing ion channel 1 at 1.9 Å resolution and low pH. *Nature* **449**, 316–323.

Johnson KO (2001). The roles and functions of cutaneous mechanoreceptors. *Curr Opin Neurobiol* **11**, 455–461.

Kang S, Jang JH, Price MP, Gautam M, Benson CJ, Gong H, Welsh MJ & Brennan TJ (2012). Simultaneous disruption of mouse *ASIC1a*, *ASIC2* and *ASIC3* genes enhances cutaneous mechanosensitivity. *PLoS One* **7**, e35225.

Kruger L, Perl ER & Sedivec MJ (1981). Fine structure of myelinated mechanical nociceptor endings in cat hairy skin. *J Comp Neurol* **198**, 137–154.

Lapatsina L, Brand J, Poole K, Daumke O & Lewin GR (2012*a*). Stomatin-domain proteins. *Eur J Cell Biol* **91**, 240–245.

Lapatsina L, Jira JA, Smith ESJ, Poole K, Kozlenkov A, Bilbao D, Lewin GR & Heppenstall PA (2012*b*). Regulation of ASIC channels by a stomatin/STOML3 complex located in a mobile vesicle pool in sensory neurons. *Open Biol* **2**, 120096.

Lechner SG, Frenzel H, Wang R & Lewin GR (2009). Developmental waves of mechanosensitivity acquisition in sensory neuron subtypes during embryonic development. *EMBO J* **28**, 1479–1491.

Lechner SG & Lewin GR (2013). Hairy sensation. *Physiology (Bethesda)* **28**, 142–150.

Lewin GR (1996). Neurotrophins and the specification of neuronal phenotype. *Philos Trans R Soc Lond B Biol Sci* **351**, 405–411.

Lewin GR, Lisney SJ & Mendell LM (1992). Neonatal anti-NGF treatment reduces the Aδ- and C-fibre evoked vasodilator responses in rat skin: Evidence that nociceptor afferents mediate antidromic vasodilatation. *Eur J Neurosci* **4**, 1213–1218.

Lewin GR & Moshourab R (2004). Mechanosensation and pain. *J Neurobiol* **61**, 30–44.

Luo W, Enomoto H, Rice FL, Milbrandt J & Ginty DD (2009). Molecular identification of rapidly adapting mechanoreceptors and their developmental dependence on Ret signalling. *Neuron* **64**, 841–856.

Martinez-Salgado C, Benckendorff AG, Chiang L-Y, Wang R, Milenkovic N, Wetzel C, Hu J, Stucky CL, Parra MG, Mohandas N & Lewin GR (2007). Stomatin and sensory neuron mechanotransduction. *J Neurophysiol* **98**, 3802–3808.

Milenkovic N, Frahm C, Gassmann M, Griffel C, Erdmann B, Birchmeier C, Lewin GR & Garratt AN (2007). Nociceptive tuning by stem cell factor/c-Kit signalling. *Neuron* **56**, 893–906.

Milenkovic N, Wetzel C, Moshourab R & Lewin GR (2008). Speed and temperature dependences of mechanotransduction in afferent fibers recorded from the mouse saphenous nerve. *J Neurophysiol* **100**, 2771–2783.

O'Hagan R, Chalfie M & Goodman MB (2005). The MEC-4 DEG/ENaC channel of *Caenorhabditis elegans* touch receptor neurons transduces mechanical signals. *Nat Neurosci* **8**, 43–50.

Page AJ, Brierley SM, Martin CM, Hughes PA & Blackshaw LA (2007). Acid sensing ion channels 2 and 3 are required for inhibition of visceral nociceptors by benzamil. *Pain* **133**, 150–160.

Page AJ, Brierley SM, Martin CM, Martinez-Salgado C, Wemmie JA, Brennan TJ, Symonds E, Omari T, Lewin GR, Welsh MJ & Blackshaw LA (2004). The ion channel ASIC1 contributes to visceral but not cutaneous mechanoreceptor function. *Gastroenterology* **127**, 1739–1747.

Page AJ, Brierley SM, Martin CM, Price MP, Symonds E, Butler R, Wemmie JA & Blackshaw LA (2005). Different contributions of ASIC channels 1a, 2, and 3 in gastrointestinal mechanosensory function. *Gut* **54**, 1408–1415.

Price MP, Lewin GR, McIlwrath SL, Cheng C, Xie J, Heppenstall PA, Stucky CL, Mannsfeldt AG, Brennan TJ, Drummond HA, Qiao J, Benson CJ, Tarr DE, Hrstka RF, Yang B, Williamson RA & Welsh MJ (2000). The mammalian sodium channel BNC1 is required for normal touch sensation. *Nature* **407**, 1007–1011.

Price MP, McIlwrath SL, Xie J, Cheng C, Qiao J, Tarr DE, Sluka KA, Brennan TJ, Lewin GR & Welsh MJ (2001). The DRASIC cation channel contributes to the detection of cutaneous touch and acid stimuli in mice. *Neuron* **32**, 1071–1083.

Price MP, Thompson RJ, Eshcol JO, Wemmie JA & Benson CJ (2004). Stomatin modulates gating of acid-sensing ion channels. *J Biol Chem* **279**, 53886–53891.

Roza C, Puel J-L, Kress M, Baron A, Diochot S, Lazdunski M & Waldmann R (2004). Knockout of the ASIC2 channel in mice does not impair cutaneous mechanosensation, visceral mechanonociception and hearing. *J Physiol* **558**, 659–669.

St John Smith E, Purfürst B, Grigoryan T, Park TJ, Bennett NC & Lewin GR (2012). Specific paucity of unmyelinated C-fibers in cutaneous peripheral nerves of the African naked-mole rat: comparative analysis using six species of Bathyergidae. *J Comp Neurol* **520**, 2785–2803.

Sluka KA, Radhakrishnan R, Benson CJ, Eshcol JO, Price MP, Babinski K, Audette KM, Yeomans DC & Wilson SP (2007). ASIC3 in muscle mediates mechanical, but not heat, hyperalgesia associated with muscle inflammation. *Pain* **129**, 102–112.

Smith ESJ, Omerbašić D, Lechner SG, Anirudhan G, Lapatsina L & Lewin GR (2011). The molecular basis of acid insensitivity in the African naked mole-rat. *Science* **334**, 1557–1560.

Stucky CL, Rossi J, Airaksinen MS & Lewin GR (2002). GFR α2/neurturin signalling regulates noxious heat transduction in isolectin B4-binding mouse sensory neurons. *J Physiol* **545**, 43–50.

Suzuki H, Kerr R, Bianchi L, Frøkjaer-Jensen C, Slone D, Xue J, Gerstbrein B, Driscoll M & Schafer WR (2003). In vivo imaging of *C. elegans* mechanosensory neurons demonstrates a specific role for the MEC-4 channel in the process of gentle touch sensation. *Neuron* **39**, 1005–1017.

Wang R & Lewin GR (2011). The Cav3.2 T-type calcium channel regulates temporal coding in mouse mechanoreceptors. *J Physiol* **589**, 2229–2243.

Wende H, Lechner SG, Cheret C, Bourane S, Kolanczyk ME, Pattyn A, Reuter K, Munier FL, Carroll P, Lewin GR & Birchmeier C (2012). The transcription factor c-Maf controls touch receptor development and function. *Science* **335**, 1373–1376.

Wetzel C, Hu J, Riethmacher D, Benckendorff A, Harder L, Eilers A, Moshourab R, Kozlenkov A, Labuz D, Caspani O, Erdmann B, Machelska H, Heppenstall PA & Lewin GR (2007). A stomatin-domain protein essential for touch sensation in the mouse. *Nature* **445**, 206–209.

Yagi J, Wenk HN, Naves LA & McCleskey EW (2006). Sustained currents through ASIC3 ion channels at the modest pH changes that occur during myocardial ischemia. *Circ Res* **99**, 501–509.

Zhang S, Arnadottir J, Keller C, Caldwell GA, Yao CA & Chalfie M (2004). MEC-2 is recruited to the putative mechanosensory complex in *C. elegans* touch receptor neurons through its stomatin-like domain. *Curr Biol* **14**, 1888–1896.

Additional information

Competing interests

None declared.

Author contributions

R.A.M., C.W., C.M.-S. and G.R.L. were responsible for the collection, analysis and interpretation of data. R.A.M., G.R.L. and C.W. drafted the article. G.R.L., R.A.M. and C.W. conceived and designed the experiments. All authors approved the final version of the manuscript.

Funding

These studies were partly supported by the Deutsche Forschungsgemeinshaft (SFB665) and a DAAD fellowship awarded to R.A.M. C.M.-S. was a recipient of a Marie Curie fellowship while collecting data for the paper.

Acknowledgements

The technical support of Heike Thränhardt and Anke Scheer is gratefully acknowledged.

Authors' present addresses

R. A. Moshourab: Department of Anesthesiology and Intensive Care Medicine, Campus Charité Mitte and Campus Virchow-Klinikum, Charité Universitätsmedizin Berlin, Campus Virchow-Klinikum, Augustenburger Platz 1, Berlin D-13353, Germany.

C. Martinez-Salgado: IECSCYL, Research Unit, IBSAL-University Hospital of Salamanca, Paseo San Vicente 58-182, 37007 Salamanca, Spain.